

This is an Open Access document downloaded from ORCA, Cardiff University's institutional repository:<https://orca.cardiff.ac.uk/id/eprint/100354/>

This is the author's version of a work that was submitted to / accepted for publication.

Citation for final published version:

Hu, Kexiang, Awange, Joseph L., Khandu, Forootan, Ehsan , Goncalves, Rodrigo Mikosz and Fleming, Kevin 2017. Hydrogeological characterisation of groundwater over Brazil using remotely sensed and model products. *Science of the Total Environment* 599-60 , pp. 372-386. 10.1016/j.scitotenv.2017.04.188

Publishers page: <http://dx.doi.org/10.1016/j.scitotenv.2017.04.188>

Please note:

Changes made as a result of publishing processes such as copy-editing, formatting and page numbers may not be reflected in this version. For the definitive version of this publication, please refer to the published source. You are advised to consult the publisher's version if you wish to cite this paper.

This version is being made available in accordance with publisher policies. See <http://orca.cf.ac.uk/policies.html> for usage policies. Copyright and moral rights for publications made available in ORCA are retained by the copyright holders.

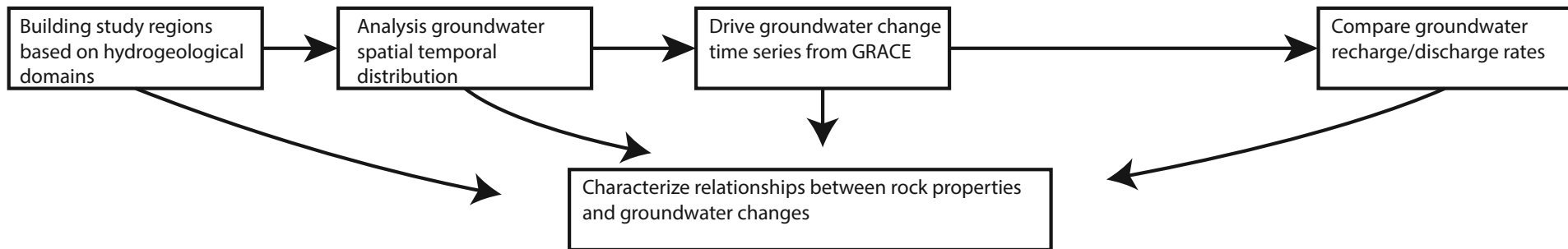
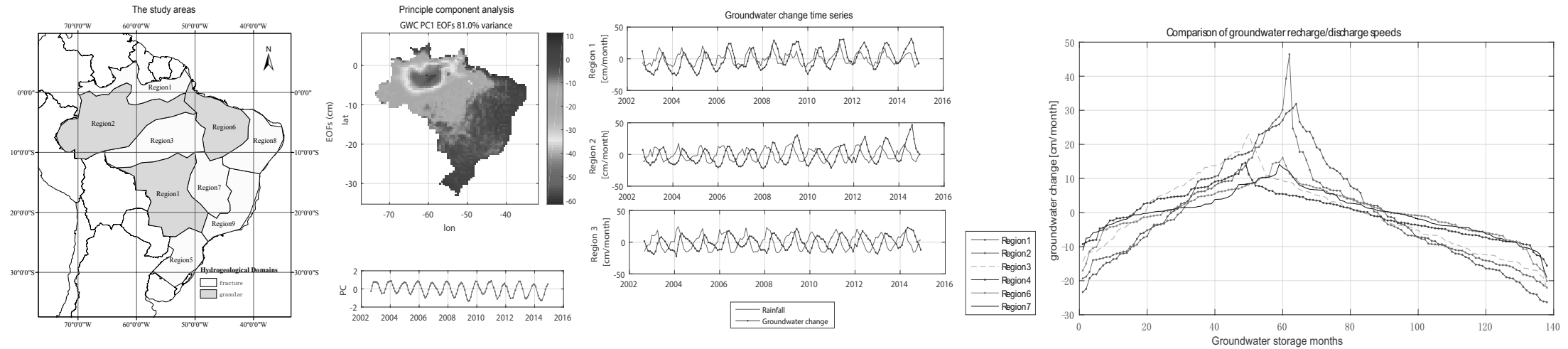


Title: Hydrogeological characterisation of groundwater over Brazil using remotely sensed and model products

Science of The Total Environment, Volumes 599–600, 1 December 2017, Pages 372–386

<http://www.sciencedirect.com/science/article/pii/S0048969717310331>

Cite as: Hu et al. 2017, Science of The Total Environment, Volumes 599-600, Pages 372–386, doi:10.1016/j.scitotenv.2017.04.188



Highlights

1. Groundwater storage changes estimated from GRACE link geological properties;
2. Rock properties controls groundwater distribution, flow rate and storage capacity;
3. The Amazon area has the largest groundwater change as well as groundwater storage;
4. The dam pattern in Amazon with groundwater >0.75 inflow and <0.45 outflow rates;
5. Wet seasons in in the Amazon regions only occupy about only 36 to 47% of all time.

Hydrogeological characterisation of groundwater over Brazil

H Kexiang^a, Joseph L. Awange^a, Khandu^a, Ehsan Forootan^b, Rodrigo Goncalves^c, Kevin Fleming^d

^a*Western Australian Centre for Geodesy and The Institute for Geoscience Research, Curtin University, Perth, Australia*

^b*School of Earth and Ocean Sciences, Cardiff University, Cardiff, UK*

^c*Department of Cartographic Engineering, Geodetic Science and Technology of Geoinformation Post Graduation Program, Federal University of Pernambuco (UFPE), Recife, PE, Brazil*

^d*Centre for Early Warning Systems, GFZ German Research Centre for Geosciences, Potsdam, Germany*

Abstract

1 Groundwater is a valuable source of freshwater across many parts of Brazil, and particularly
2 during the times of prolonged-droughts. While groundwater storage in Brazil is largely affected
3 by precipitation variations (e.g., severe droughts), we show that groundwater storage changes
4 estimated using GRACE time-variable gravity field solutions and hydrological model outputs
5 (such as GLDAS and WGHM) respond to the spatially varying geological settings across the
6 country. The impacts of precipitation variability were also taken into account to carefully study
7 groundwater storage variations under different geological settings in Brazil. The results indicate
8 that climate variability mainly control groundwater change trends while geological properties
9 control change rates, spatial distribution, and storage capacity. Granular rocks in the Amazon
10 and Guarani aquifers are found to influence larger storage capability, higher permeability (> 104
11 m/s) and faster response to rainfall (1–3 months lag) compared to fractured rocks (permeability
12 < 107 m/s and > 3 months lag) found only in Bambui aquifer. Groundwater in the Amazon
13 region is found to rely not only on precipitation but also on inflow from other regions. Areas
14 beyond the northern and southern Amazon basin depict a dam-like behaviour, with high inflow
15 and slow outflow rates (recharge slope > 0.75 , discharge slope < 0.45). This is due to two
16 impermeable rock layer-like walls (permeability ≤ 108 m/s) along the northern and southern
17 Alter do Chão aquifer that helps retain groundwater. The largest groundwater storage capacity
18 in Brazil is the Amazon aquifer (with annual amplitudes of > 30 cm). Amazon's groundwater
19 declined from 2002–2008 due to below normal precipitation (wet seasons lasted for about 36–
20 47% of the time). The Guarani aquifer and adjacent coastline areas rank second in terms of

21 storage capacity, while the northeast and southeast coastal regions indicate the smallest due to
22 lack of rainfall (annual average is rainfall < 10 cm).

Keywords: Brazil, groundwater changes, hydrogeology, rock properties, GRACE

23 1. Introduction

24 Groundwater is a very important resource that supports daily life (Cameron, 2012). Globally,
25 about 97% of the Earth's water exists in the ocean and only 3% on land. Of this amount, 0.61%
26 consists of groundwater, 0.01% surface water (e.g., lakes and rivers), and the remaining 2.38%
27 is contained in ice sheets and caps, glaciers, and soil moisture (Harter, 2001). Groundwater,
28 by contrast to surface water, has the advantage of water storage volume and is usually cleaner
29 than surface water due to the fact that filtration through the soil helps to purify the incoming
30 water.

31 In Brazil, a developing country rich in surface water (i.e., the Amazon river), about 16%
32 of the population rely exclusively on groundwater, which also acts as perennial sources to its
33 bountiful surface water resources across the country (Hirata and Conicelli, 2012). Although
34 Brazil is believed to have nearly a fifth of the world's water resources, water shortage problems
35 still bedevilled most of its states, a situation that is set to continue for a long time in light
36 of frequent droughts. For example, São Paulo and Rio de Janeiro recently (2014 to 2015)
37 experienced the worst drought in the last 80 years (Otto et al., 2015; Awange et al., 2016).
38 Other areas, such as northeastern Brazil and the Amazon River Basin, also suffer from frequent
39 droughts (e.g., Lemos et al., 2002; Rowland et al., 2015).

40 Numerous studies (e.g., Negri et al., 2004; Vieceli et al., 2015) have tried to understand
41 water shortage problems and frequent occurrences of droughts by assessing the relationship
42 between water storage changes (e.g., lakes and rivers) and hydro-meteorological parameters
43 such as precipitation, temperature and vegetation coverage. However, only a few of these
44 studies, (e.g., Bahniuk, 2008) managed to link them to subsurface properties such as rock
45 permeability and layer structure. The spatial distribution of various geological characteristics
46 and conditions (i.e., rock types and elevation) could be critical factors for understanding the
47 nature of groundwater storage behaviour across Brazil (e.g., Zagonari, 2010).

48 In fact, from a geological perspective, precipitation controls groundwater changes through
49 its seasonal and annual variations, providing the main source of water, and when rainfall varies,

50 groundwater follows. Furthermore, i.e., generally speaking, when rain falls to the surface, it
51 takes time to infiltrate the ground and become groundwater. The speed of fluid moving in rocks
52 is limited by the size and number of pores, fractures, and permeability of rocks (Farlin et al.,
53 2013). In addition, rock properties also influence the capacity of storing groundwater in rock
54 layers due to the limitations in space (pores and fractures) for storing water.

55 To date, most studies that have focused on groundwater in Brazil use isotopic measurements
56 (e.g., Marimon et al., 2013; Mendonca et al., 2005; Gastmans, 2016), which put radioactive
57 isotopic atoms into a part of water cycle, i.e., hydrogen in water (H_2O), and trace the radiations
58 in order to detect the groundwater distribution and availability. It is an accurate method for
59 studying groundwater distribution and availability, but is rather expensive and requires, skilled
60 experts and long study period (see e.g., Soler and Bonotto, 2015). Usually, such a method is
61 used to achieve a detailed understanding of the functioning of an aquifer in the area of a well
62 field, and is therefore difficult to apply over large study area.

63 Also, climatic characteristics (e.g., Broad et al., 2007; Norbre et al., 2016) are usually
64 used to predict and evaluate drought episodes. However, they rarely link groundwater to
65 their geological properties and as such, does not offer new information on potential source
66 of water. Other techniques, such as geothermal methods (e.g., Pimentel and Hamza, 2014),
67 electromagnetic methods (e.g., Filho et al., 2010) and statistical flow models (e.g., Friedel et
68 al., 2012) also have been partly applied to infer on the relationship between groundwater and
69 geological properties (including rock categories) across Brazil, but have been restricted to small
70 scale characterizations due to the limitation of cost and time.

71 To address these drawbacks, this study utilizes remotely sensed time-variable gravity field
72 products of the Gravity Recovery and Climate Experiment (GRACE, Tapley et al., 2004) mis-
73 sion to estimate total water storage (TWS) changes over Brazil (see, e.g., Getirana, 2015; Melo
74 et al., 2016; Ferreira et al., 2012) . For this, we follow the signal separation approach (e.g., in
75 Xiao et al., 2015; Cao et al., 2015; Zheng and Chen, 2015; Castellazzi et al., 2016; Forootan
76 et al., 2014), and remove other forms of water storage (surface water, soil moisture, canopy
77 water) obtained from models/observations from GRACE TWS. GRACE has already proven
78 to be a viable technique for monitoring TWS changes (e.g., Han et al., 2009; Abelen et al.,
79 2015; Sinha et al., 2016). Also, Awange et al. (2014) used GRACE TWS to characterize mega
80 hydrogeological regimes of Ethiopian, thus showcasing the capability of GRACE products to be

81 linked to geological properties. However, to the best of the authors' knowledge, no study has
82 attempted to use GRACE products to investigate the relationship between groundwater storage
83 changes and geological properties in Brazil. Knowledge of groundwater relationships to geolog-
84 ical characteristics is desirable for understanding aquifer water storage, and recharge/discharge
85 characteristics. Such knowledge is important for making decisions in water management and
86 utilization.

87 To complement previous efforts of hydrogeological characterization of groundwater over
88 Brazil, this study investigates the relationships between groundwater changes and rock prop-
89 erties by (i) deriving groundwater through subtracting soil moisture, canopy water and surface
90 water from TWS, (soil moisture and vegetation or canopy water storage can be estimated
91 from GLDAS (Global Land Data Assimilation System)) (Rodell et al., 2004) products, sur-
92 face water storage from WGHM (WaterGAP Global Hydrology Model version 2.2a (Döll et al.,
93 2014; Müller Schmeid et al., 2014)) and various satellite altimetry missions (e.g., Cretaux et
94 al., 2011)'s products, (ii) employing geological data such as rock layer distribution, elevation,
95 aquifer types to understand the Brazilian geological conditions, (iii) estimating the impacts
96 of rainfall on the Brazilian groundwater changes using TRMM (Tropical Rainfall Measuring
97 Mission) (TMPA, Huffman and Bolvin, 2015) data sets, and (iv) combining (i) and (ii) to
98 characterise groundwater change behaviours in different rock formations. This is because rock
99 formations with specific properties could lead to large groundwater storage potential.

100 The study is organised as follows. In Section 2, the hydrogeological characteristics of Brazil-
101 ian aquifers, which provides the necessary perspective to characterize the GRACE-derived
102 groundwater changes is presented. Section 3 then provides the data and analysis methods
103 used in the study while the results are discussed in Section 4, with Section 5 concluding the
104 study.

105 **2. Hydrogeological characteristics of Brazilian aquifers**

106 *2.1. Study area*

107 The whole of Brazil is divided into 9 study regions based on fractured and granular rock
108 formations (Figure 1a). It can be seen that most of the aquifer systems in Brazil are located
109 within granular rock formations (Figure 1b). From Figure 1c, in North Brazil, the three main

110 aquifer systems (Solimões, Içá and Alter do Chão; Figure 1b) combine to form the Amazon
 111 aquifer (region 2). Region 4 in the Central-West (upper Paraná basin) consist of the Pantanal,
 112 Aquidauana and Bauru-Caiuá aquifers, which belong to granular rock formations. Only the
 113 Serra Geral and Bambuí aquifers in regions 4, 5 and 7 are located in fractured rocks. In
 114 addition, there are no aquifers located in regions 1 and 3 in the northern and southern sides of
 115 the Amazon aquifer, respectively, and regions 8 and 9 in the coastal areas of northeastern and
 116 southeastern Brazil, respectively. Some information on the 9 study regions are summarised in
 117 Table 1.

Table 1: Some fundamental information about the 9 study regions of Brazil (data source: CPRM, 2014; Ricardo and Bruno, 2011). Note*: The rock type for each region only represents the first rock layer under the surface.

Region	Rock type*	Aquifer	Groundwater flow direction
1	Fractured	None	North to south
2	Granular	Alter do Chão, Içá and Solimões	West to east
3	Fractured	None	
4	Granular	Bauru-Caiuá, Serra Geral, Botucatu & Piramboia, Pantanal	East to west
5	Fractured	Serra Geral and Botucatu &Piramboia	Northeast to southwest
6	Granular	Itapecuru, Piauí	South to north
7	Fractured	Urucuia and Bambuí	South to north
8	Fractured	None	West to east
9	Fractured	None	West to east

118 2.2. Geological properties linked to groundwater

119 Groundwater exists beneath the Earth's surface stored in rock pore spaces and fractures
 120 (Nelson, 2015). Although precipitation is the main factor that controls the replenishment of
 121 groundwater, and hence its changes, it is also strongly influenced by rock properties in different
 122 areas. In Brazil, groundwater is stored in two types of rocks, granular and fractured rocks
 123 (Figure 1a). The basic difference between these two types of rocks is the way in which water

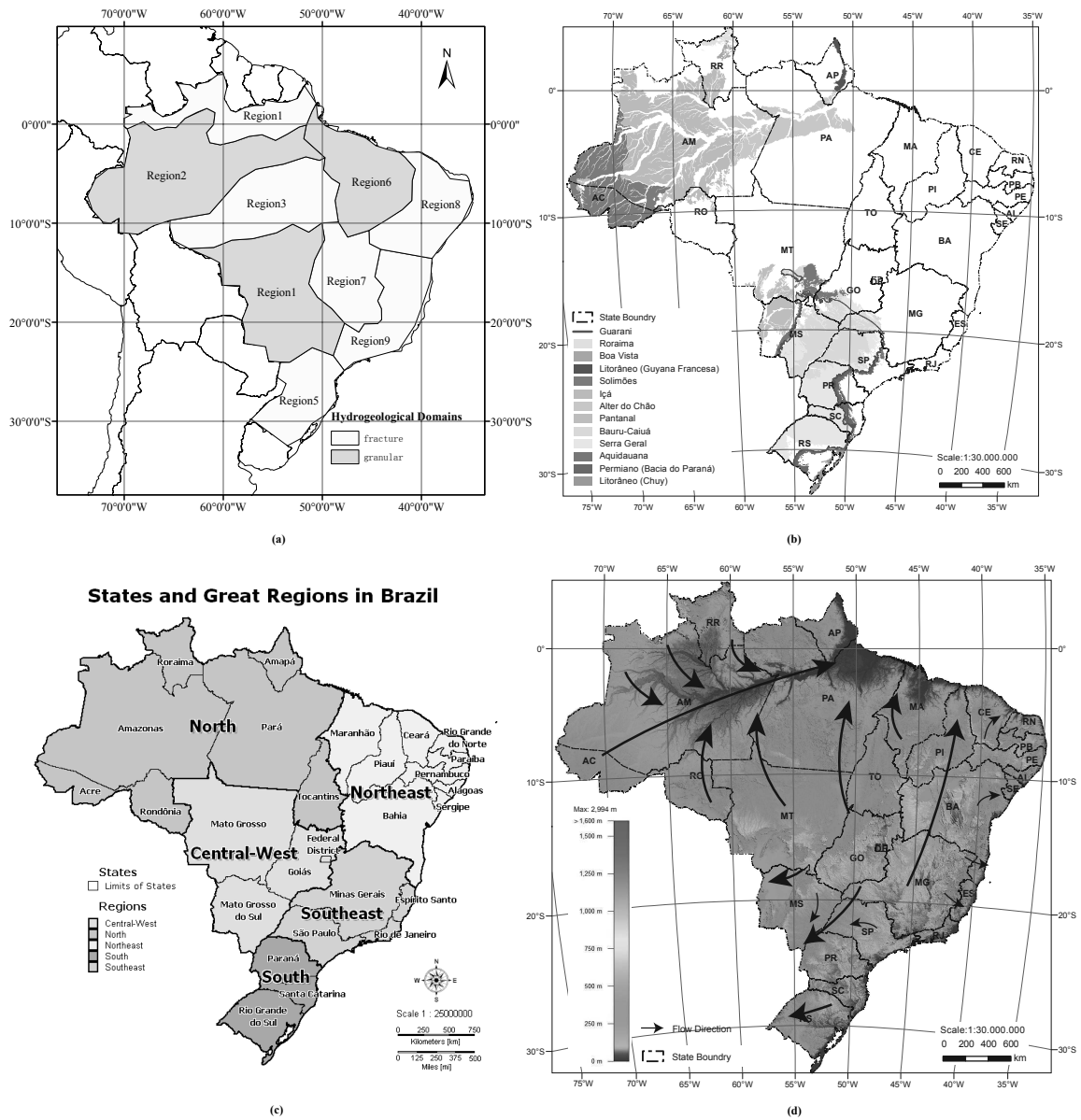


Figure 1: (a) The study areas, (b) the main aquifer systems in Brazil, (c) states and great regions in Brazil, and (d) elevation and general groundwater/surface water flow direction map over Brazil (data source: modified from CPRM, 2014)

124 is stored. Fractured rocks store water in gaps while the granular rocks store water in pore
 125 spaces (CPRM, 2014; Ricardo and Bruno, 2011). Granular rocks in Brazil mainly include sand,

126 clay, silt, sandstone and conglomerate, and partly contain limestone and dolomite (CPRM,
127 2014; Ricardo and Bruno, 2011). Fractured rocks mainly consist of basalt, diabase, and mixed
128 rocks (mixed with granitoid, volcanic and metamorphic rocks). There are also some areas
129 (i.e, Bambui aquifer) covered by karst, which is a very special topography that is made up of
130 creviced rocks with extremely well developed fractures. To understand the GRACE-derived
131 groundwater behavior in Brazil, the following properties are defined:

132 (i) ‘Porosity’ refers to voids within a rock, and directly determines groundwater storage
133 capacity. Loose, incompact rocks will have more pore spaces than consolidated rocks. Some
134 rocks, such as igneous and metamorphic, may have no pore spaces, but could have open spaces
135 due to fractures. In general, rocks with pore spaces are usually granular, which are permeable
136 (water can directly pass through) and provide more stable conditions (higher porosity) for
137 water transport compared to fractured rocks. Fractured rocks are impermeable, that is, water
138 cannot directly pass through, but only flows via the fractures. Due to the fact that fractures are
139 not usually distributed homogeneously like pore spaces in rocks, some regions have continuous,
140 perforated fractures, while others do not. Thus, granular rocks provide more desirable properties
141 for the storage of groundwater than fractured rocks.

142 (ii) ‘Permeability’ is another important concept, which refers to groundwater flow rates
143 inside the rocks. Nelson (2015) pointed out that an aquifer is a large body of permeable ma-
144 terial where groundwater can easily move through via pore space or fractures. According to
145 different permeability levels, different rock formations are divided into aquifers (high perme-
146 ability), aquitards (low permeability) and non-aquifers (almost zero permeability). The higher
147 permeability of a rock formation not only represents a larger potential capacity for storage of
148 groundwater (more pore space or fractures to store water), but also means a weaker ability to
149 hold groundwater, i.e., groundwater flows in and out quickly.

150 (iii) ‘Elevation’. Groundwater table level variation usually follow the trend in terrain fluc-
151 tuation, i.e., high elevation areas usually have higher levels of groundwater table than lower
152 elevation areas (Charles and William, 2001). Furthermore, groundwater flow directions follow
153 the principle of hydraulic gradient (i.e., flow from high gradients to low gradients) (Freeze and
154 Witherspoon, 1967). Figure 1d summarises the surface/groundwater flow directions over Brazil
155 based on elevation, which can be categorised into three main parts: the north (Amazon), the
156 centre-west and south parts (Paraná), and the northeastern and southeastern coastal areas of

157 Brazil. First, the centre line of groundwater flow direction in the northern part follows the
158 Amazon River, which is from west to east. The groundwater flow directions of the areas north
159 and south of the Amazon basin both point towards the Amazon River. Second, the elevation
160 distribution of the Paraná basin is high to low from the northeast to the southwest, hence, the
161 groundwater flow direction. As for the coastal areas, most are split from inland by the Pico da
162 Bandeira mountain. Groundwater then flows into the Atlantic Ocean from west to east.

163 *2.3. Aquifer identification*

164 Groundwater changes are usually associated with multiple rock layers and aquifer types,
165 which may represent different rock formations and their properties. This makes it challenging
166 to relate groundwater changes to a single rock formation. It is therefore necessary to identify the
167 rock formation(s) and aquifer(s) (together with their properties) that contribute to groundwater
168 changes in Brazil.

169 Aquifers can be of two types, generally, (i) unconfined, where the water table is exposed to
170 the Earth's atmosphere through the unsaturated zone and (ii) confined, where it is completely
171 filled with water and separated from the surface by an overlying aquitard or almost impermeable
172 rock layer. Theoretically, due to the fact that groundwater in an unconfined aquifer can be
173 quickly replenished by rainfall (direct recharge mechanism), the water table varies from season
174 to season. By contrast, the groundwater changes in confined aquifers are relatively small and
175 do not suffer from seasonal changes since the aquifer can only be recharged via slow infiltration
176 (indirect recharge mechanism) from the overlying aquitards or almost impermeable rock layers.
177 Therefore, groundwater storage changes derived from GRACE will largely represent changes in
178 unconfined aquifers.

179 Figure 1b shows the main aquifer systems over Brazil, which are defined only by the first rock
180 formation under the Earth's surface. According to Alisson (2014), the largest two groundwater
181 reservoirs in Brazil are the Amazon and Guarani aquifers, which represent more than 80% of
182 the total water storage in the Amazon and Paraná basins.

183 The Amazon aquifer, located in northern Brazil, consists of the Solimões, Içá and Alter do
184 Chão aquifer systems from west to east (Figure 2a). Figures 2c and 2d give a cross section of
185 the Solimões to Içá (A-A') and Alter do Chão aquifer systems (B-B'), respectively. It is clear
186 that the Içá is the thinnest unconfined aquifer system above Solimões and Alter do Chão. The

187 semi-unconfined Solimões is half exposed to the west, while the other half is under the Içá. As
188 for the biggest semi-unconfined Alter do Chão aquifer system, one third of its outcropping is in
189 the Amazon basin and the rest of it is under the Solimões and Içá aquifer systems. With regards
190 to the groundwater volume capacity, the groundwater storage of the Içá and Solimões (7,200
191 km³) are only 22% of the Alter do Chão aquifer system (33,000 km³). Therefore, the Alter do
192 Chão is the main aquifer system that contributes to groundwater changes in the Amazon basin.
193 The rock formation characteristics and hydraulic features of the Alter do Chão, Solimões and
194 Içá are presented in Table 2.

195 Compared to the Amazon aquifer, the geological conditions of the Guarani (2b) are much
196 more complex due to the fact that it is located over areas ranging from mountains to basins.
197 Figure 2b only gives a very general overview of the horizontal distribution of the components
198 of the Guarani aquifer system and shows the vertical structure of three aquifer systems, the
199 Bauru (the 1st rock formation), the Serra Geral (the 2nd rock formation) and the Botucatu and
200 Piramboia (the 3rd rock formation). More detailed information can be found in, e.g., CPRM
201 (2014). Following Ondra (2002), the formation characteristics and hydraulic features of the
202 Bauru, Serra Geral, Botucatu and Piramboia are presented in Table 2. From a thickness point
203 of view, the Serra Geral varies a great deal, ranging from 20 m to 1,200 m from one area to
204 another. The Botucatu and Piramboia have an average thickness of 500 to 600 m, while the
205 Bauru is only about 200 m in thickness on average. Obviously, the Botucatu and Piramboia
206 rock formations make up the biggest part of groundwater volume with the highest permeability.
207 The Serra Geral layer also consists of a large part of the Guarani aquifer system, however, the
208 fractured rocks do not have so much space to store water. Hence, the Botucatu and Piramboia
209 mainly control groundwater changes in the Guarani aquifer.

210 *2.4. 'Dam' and 'basin' reservoirs patterns*

211 Sometimes, for an area with a specific elevation and rock layer distribution, a new structure
212 will be formed, which exerts a major influence on groundwater storage and change. 'dam' and
213 'basin' reservoirs patterns are two such structures established to influence groundwater over
214 Brazil in this study.

215 First, there are two impermeable rock layers like 'walls' standing at the northern and south-
216 ern sides of the edges of the Alter do Chão (see Figure 2a), which consist of basalt, diabase, and

Table 2: Rock type descriptions of the Amazon and Guarani aquifers, together with their hydraulic features (data source: CPRM, 2014; Ondra, 2002; Eliene et al., 2013).

Stratigraphic Formation	Aquifer type	Rock type	Rock component	Permeability (m/s)	Water storage identification
Amazon aquifer system					
Içá	unconfined	granular	fine to medium sandstones and siltstones	1×10^{-5} to 1×10^{-6}	small
Solimões	semi-unconfined	granular	greenish argillaceous sandstones	5×10^{-5} to 1×10^{-6}	small
Alter do Chão	semi-unconfined	granular	coarse and friable sandstones	2.1×10^{-4} to 5.0×10^{-5}	large
Guarani aquifer system					
Bauru	unconfined	granular	sandstone with quartz dominant and carbonatic	1×10^{-5} to 1×10^{-6}	small
Serra Geral	semi-unconfined	fractured	sandstone with quartz dominant and carbonatic	5×10^{-5} to 5×10^{-7}	small
Botucatu & Piramboia	semi-unconfined	granular	aeolian sandstone with quartz plus feldspars	1.5×10^{-4}	large

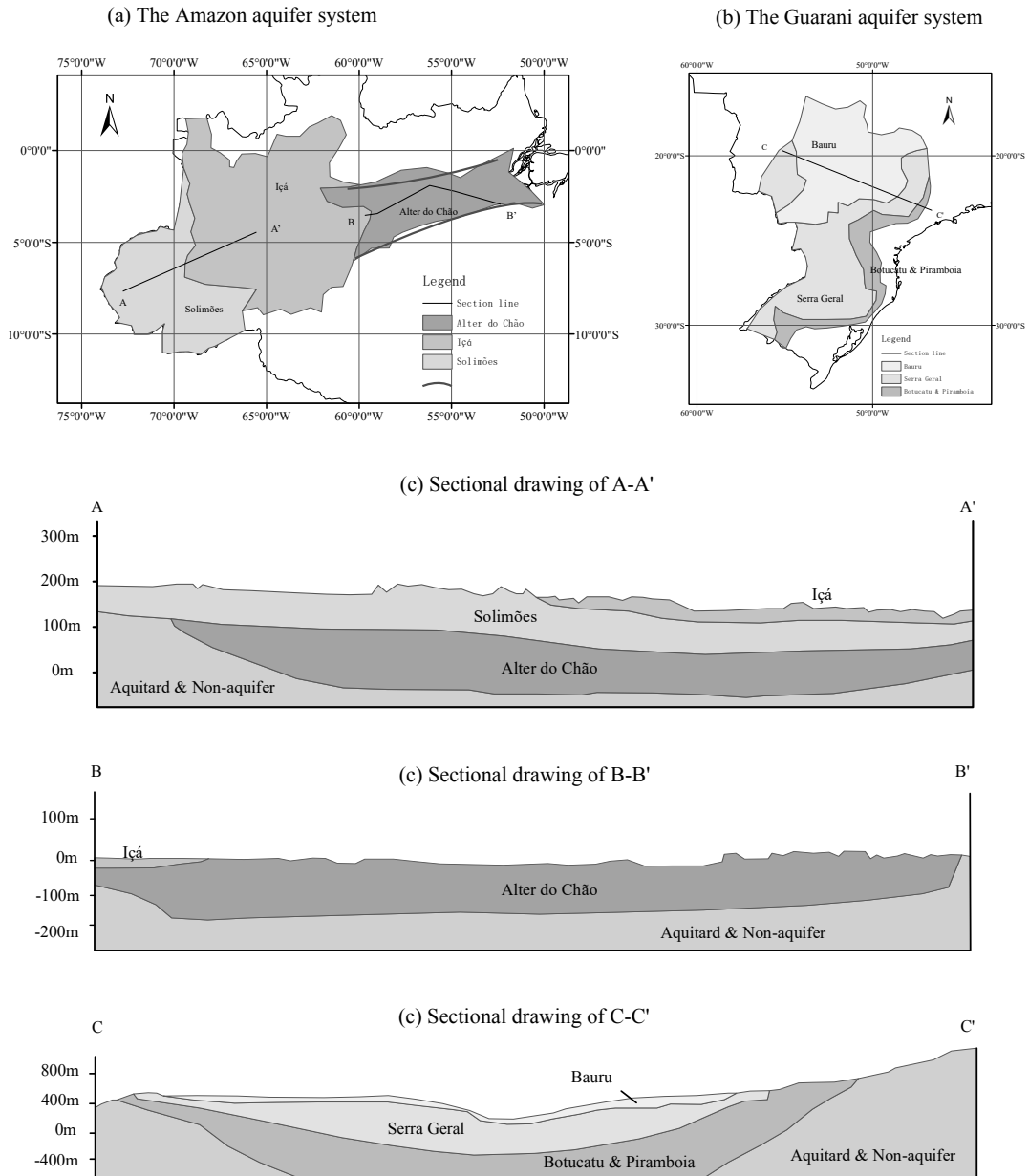


Figure 2: (a) The Amazon aquifer system. (b) The Guarani aquifer system. (c) Sectional drawing of the Solimões, Içá. (d) Sectional drawing of the Alter do Chão. (e) Sectional drawing of the Guarani aquifer system (data source: modified from CPRM, 2014)

217 mixed rocks. Detailed information can be found in the geology map of CPRM (2014). From

218 Figure 1d, one can see that groundwater and surface water are converging from areas beyond
219 the north and south of the Amazon basin. However, when groundwater meets the northern and
220 southern edges of the Alter do Chão, they hit the ‘walls’. These two impermeable rock layers
221 with permeability less than 1×10^{-8} m/s slows the groundwater flow into the Amazon basin
222 to a large extent. Hence, the groundwater gathers near these two edges like dams retaining
223 water. Thus, a large volume of groundwater storage can be expected in areas to the northern
224 and southern sides of the Amazon basin if there is enough rainfall as a source of groundwater.

225 Second, the Guarani aquifer system is a very good example of the ‘basin’ reservoir pat-
226 tern. Figure 2e shows the structures of the two main Guarani aquifer systems in the west-east
227 direction, the Serra Geral, and the Botucatu and Piramboia, which lie in a ‘U’ shape. The
228 groundwater flow direction in the Guarani aquifer system is therefore from two sides towards
229 the middle, and the groundwater changes depend to a large extent on the size of the direct
230 recharge area, which is very small at the two sides of the Guarani aquifer (outcrops of Serra
231 Geral, Botucatu and Piramboia, see Figure 2b). However, due to the Paraguay Paraná plain
232 being located to the east of the Guarani aquifer, the run-off speed of groundwater from the
233 northwestern to southeastern direction will be slow, which making it possible for the Guarani
234 aquifer with small direct recharge areas to gather groundwater slowly if there is enough rain-
235 fall as a source of groundwater. Stable groundwater storage and changes (both spatially and
236 temporally), therefore, will be expected in the Guarani aquifer.

237 *2.5. Indicators of large potential groundwater storage capacity*

238 The contents of the hydrogeological characteristics above and the expected relationships
239 between rock properties and groundwater behavior are summarised in Table 3. They provide
240 the basic characteristics for comparison and evaluation of the results derived from remotely
241 sensed GRACE and TRMM products, together with the WGHM and GLDAS model outputs.

242 **3. Data and methodology**

243 *3.1. Data*

244 Various satellite-based and hydrological model data sets are employed in this study to in-
245 vestigate the relationship between changes and rock properties. The data sets are summarised
246 in Table 4

Table 3: Geological characteristics linked to groundwater changes.

Geological characteristics	Relationships with respect to groundwater changes
Granular rock type	Stable transmitting conditions and large storage potential.
High permeability	Large storage potential, but weak retaining capability.
Unconfined aquifer	Large storage potential and direct recharge mechanism.
‘Dam’ reservoir	High groundwater increasing speed, but slow outflow speed.
‘Basin’ reservoir	Storage and changes depend on the size of the recharge areas.

247 *3.1.1. GRACE*

248 The Gravity Recovery and Climate Experiment (GRACE) satellites were designed and
 249 launched by the National Aeronautics and Space Administration (NASA) and the German
 250 Space Agency (DLR) to detect changes in the Earth’s gravity field. GRACE consists of twin
 251 satellites moving at low altitude orbits of 300 to 500 km (Tapley et al., 2004) with an ability to
 252 detect water changes of about 0.9 mm (Andersen et al., 2005). For an accuracy of millimeters
 253 level in TWS derived from GRACE to be achieved, the basin sizes should be greater than its
 254 spatial resolution is more than 200,000 km² (see, e.g., Zhiyong et al., 2015; Tapley et al., 2004).

255 For this study, GRACE products (LR05: Release-05 GRACE Level-2 product) are ob-
 256 tained from the CSR (University of Texas Center for Space Research) centre ([http://www.csr.
 257 utexas.edu/grace/RL05.html](http://www.csr.utexas.edu/grace/RL05.html)). The data are processed based on the approaches of Wahr et
 258 al. (1998); Swenson and Wahr (2006); Jekeli (1981) using a Gaussian filter of radius 300 km
 259 (Jekeli, 1981) to remove the noise. GRACE products provides a map of the Earth’s gravity
 260 changes, which can be converted to water equivalent height (TWS). For a consistent comparison
 261 with the gridded GLDAS data sets as well as reducing the leakage error by the filters, GRACE
 262 data is converted from 1° × 1° to 0.5° × 0.5° resolution and multiplied by a gridded scale factor
 263 derived from the GLDAS TWS following Landerer and Swenson (2012).

264 *3.1.2. TRMM*

265 The Tropical Rainfall Measurement Mission (TRMM, Kummerow et al., 1998) is a collab-
266 orative effort between NASA and the Japanese Aerospace Exploration Agency (JAXA). The
267 satellite was launched in 1997 into a near circular orbit of approximately 350 km with a period
268 of 92.5 minutes. Here, we use the monthly gridded product TRMM 3B43 that are generated
269 by the TRMM Multi-satellite Precipitation Analysis (TMPA, Huffman and Bolvin, 2015). The
270 monthly TRMM 3B43 products, hereafter as TRMM, are provided at a spatial resolution of
271 $0.25^\circ \times 0.25^\circ$ and can be obtained from [https://pmm.nasa.gov/data-access/downloads/
272 trmm](https://pmm.nasa.gov/data-access/downloads/trmm)). To be consistent with GRACE-derived TWS, the TRMM derived values are converted
273 to $0.5^\circ \times 0.5^\circ$.

274 *3.1.3. GLDAS*

275 The Global Land Data Assimilation (GLDAS) was developed by NASA Goddard Space
276 Flight (GSFC), the National Oceanic Atmospheric Administration (NOAA) and the National
277 Centre for Environmental Prediction (NCEP) (Rodell et al., 2004; Hualan and Hiroko, 2016;
278 Zheng and Chen, 2015). It provides land surface fluxes with a 3 hours and monthly temporal
279 resolution, and two spatial resolutions, 1° and 0.25° . There are four types of Land Surface
280 Models (LSM) that GLDAS concentrates on; i.e., MOSAIC, NOAH, CLM and VIC. In this
281 study, NOAH LSM data (obtained from <http://disc.sci.gsfc.nasa.gov/uui/datasets>)
282 with a spatial resolution of $0.25^\circ \times 0.25^\circ$ are applied to derive soil moisture and canopy water
283 variations. To be consistent with GRACE, GLDAS data sets are processed in the same manner
284 and converted to $0.5^\circ \times 0.5^\circ$ resolution using the same scale factor as with GRACE.

285 *3.1.4. WGHM*

286 The WaterGAP Global Hydrology Model (WGHM) simulates the continental water cycle
287 using conceptual formulations for the most important hydrological processes (Werth and Gunt-
288 ner, 2010; Döll et al., 2014). In this study, WGHM provides data sets of global TWS, soil
289 moisture, canopy, reservoirs, lakes and groundwater storage, with a spatial resolution of 0.5°
290 $\times 0.5^\circ$, which are used to evaluate the groundwater changes derived from GRACE. Besides,
291 WGHM groundwater model variants IRR_70_S (deficit irrigation at 70% of optimal irrigation
292 with groundwater recharge from surface bodies) and NOUSE_S (no water use at all assumed
293 with groundwater recharge from surface bodies) are used to evaluate the human consumption

294 of groundwater.

295 3.1.5. Satellite altimetry

296 Water level fluctuations provided by altimetry missions can be used to monitor surface water
297 reservoirs (e.g., river and lakes) height variations at global and regional scales (see, e.g., Awange
298 et al., 2013; Tarpanelli et al., 2013; Paiva et al., 2013). Available products from Topex/Poseidon,
299 Jason 1 and 2, and Envisat satellites are obtained from: <http://www.legos.obs-mip.fr/>. In
300 this study, monthly lake variations are used to estimate surface water storage changes for Lakes
301 Balbina, Tucuruí, and other main 6 lakes (reservoirs) in Brazil.

Table 4: Summary of the data sets used in this study.

Data	Period	Temporal resolution	Spatial resolution	References
GRACE	2002-2015	Monthly	$1^\circ \times 1^\circ$	Tapley et al. (2004)
TRMM	2002-2015	Monthly	$0.25^\circ \times 0.25^\circ$	Kummerow et al. (1998)
GLDAS	2002-2015	Monthly	$0.25^\circ \times 0.25^\circ$	Rodell et al. (2004)
WGHM	2002-2015	Monthly	$0.5^\circ \times 0.5^\circ$	Döll et al. (2014)
Altimetry	2002-2015	10-days		Cretaux et al. (2011)

302 3.2. Methodology

303 3.2.1. Groundwater changes derived from GRACE

304 Groundwater changes can be computed as:

$$\Delta GW = \Delta TWS - \Delta SM - \Delta CW - \Delta SW, \quad (1)$$

305 where ΔGW are the groundwater changes, ΔTWS the total water storage changes, ΔSM the
306 soil moisture changes, ΔCW the canopy water changes and ΔSW the surface water changes.
307 ΔTWS are obtained from GRACE, while ΔSM and ΔCW are derived from GLDAS (see e.g.,
308 Haohan et al., 2013; Nanteza et al., 2016). As for ΔSW , many previous studies that computed
309 GRACE-derived groundwater changes (e.g., Awange et al., 2014; Haohan et al., 2013) do not

310 consider surface water, given that they were often too small in their respective study areas.
311 For Brazil, however, due to a large number of rivers and lakes located within the different
312 regions of study, ΔSW might be a significant part of ΔTWS and could cause bias when we
313 make conclusion without removing it. Therefore, it is necessary to calculate surface water
314 contribution (rivers and lakes need to be estimated separately) for each region, and test how
315 much influence it will bring to ΔGW . In fact, the lake water storage changes and river water
316 storage changes in most regions of the Brazil can be ignored, only the Amazon basin (region
317 2) with large river water storage needs to be removed. The computations and results can be
318 found in the Supporting Material (Section A). Here we only present the results of groundwater
319 storage change time series for the Amazon basin, before and after removing the river water
320 storage changes.

321 Figure 3a shows a river water storage distribution map over Brazil estimated using WGHM,
322 while Figure 3b is a filtered version of Figure 3a after removing all the pixels consisting of water
323 storage values smaller than the 300 mm. The 300 mm value was tested along side 100 mm and
324 200 mm, and was finally selected as a threshold to distinguish the differences between large
325 rivers and small streams. It is easily seen that the Amazon river is the main contributor of
326 surface water storage in region 2 (see Figure 1a). River water storage in the rest of the study
327 regions were ignored since they are relatively small (i.e., contributions to time series of less than
328 0.5 cm). Figure 4 presents a comparison of the GRACE-derived groundwater storage changes
329 (ΔGW) before and after removing the river water storage changes, and WGHM-derived ΔGW
330 in region 2. The results show that the amplitude of the GRACE decreased by about 5 to 10 cm
331 after removing the river water storage. However, there is still a significant difference between
332 GRACE and WGHM-derived ΔGW values in region 2. With such a difference in groundwater
333 changes in region 2 derived by the two different products (GRACE and WGHM), it raises the
334 issue of the accuracy of the used data sets. In the Supporting Material (Section B), a detailed
335 evaluation of the two data sets is carried out.

336

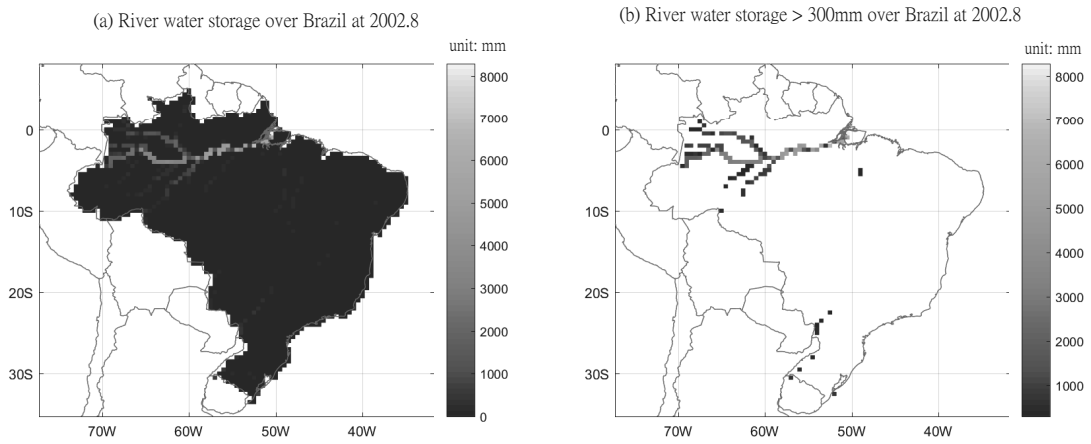


Figure 3: (a) River water storage map estimated by WGHM. (b) River water storage map filtered by removing areas less than 300mm. This is undertaken to filter out insignificant contributions from small rivers.

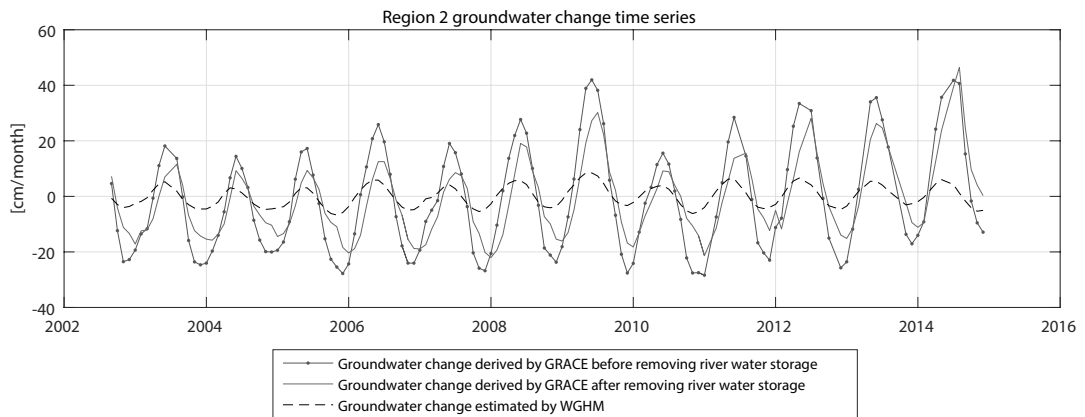


Figure 4: Region 2's groundwater changes derived from GRACE and WGHM products. After removing the surface water, the groundwater derived by GRACE decreased by 5 to 10 cm (i.e., the red line).

337 *3.2.2. Principle component analysis (PCA)*

338 Principal component analysis (PCA; Preisendorfer (1988)), widely applied in meteorology, is
 339 a method employed to a group of time series data to reduce the dimension of multivariate data
 340 in order to extract the most dominant variations in the original data set through the creation
 341 of new variables with linear functions. Assuming a data matrix $x_{i,k}$ contains rows representing

342 the time i (in months or days) and k , given k variables at a given time period i , the linear
 343 combination for k principal components (PCs) is given by (Preisendorfer, 1988):

$$PCs = \begin{pmatrix} y_{i,1} = p_{11}x_{i,1} + p_{12}x_{i,2} + p_{13}x_{i,3} + \dots + p_{1k}x_{i,k} \\ y_{i,2} = p_{21}x_{i,1} + p_{22}x_{i,2} + p_{23}x_{i,3} + \dots + p_{2k}x_{i,k} \\ \dots \\ y_{i,k} = p_{k1}x_{i,1} + p_{k2}x_{i,2} + p_{k3}x_{i,3} + \dots + p_{kk}x_{i,k} \end{pmatrix}, i = 1, 2, \dots, n, \quad (2)$$

344 where y values are orthogonal PCs that explain variability from high ($y_{i,1}$) to low ($y_{i,k}$). The
 345 eigenvalues ($\lambda_1, \lambda_2, \dots$) corresponds to each eigenvector ($p_{1,1}, p_{1,2}, \dots$), which explains the
 346 fraction of the total variance explained by the loadings (p). Further details can be found, e.g.,
 347 in Preisendorfer (1988). In this study, the empirical orthogonal functions (EOFs) derived from
 348 matrix $x_{i,k}$ give EOF/PC pairs, are called PCA modes. The output of a PCA decomposition
 349 give the trends and dominant spatio-temporal patterns of TWS, rainfall, and groundwater to
 350 help evaluate the impact of rainfall on groundwater changes.

351 3.2.3. Box plot analysis

352 A box plot can be a convenient way of graphically depicting numerical data variability
 353 (Rousseeuw et al., 1999), and indicates values of the maximum, minimum, medium and 1st
 354 (i.e., 25%), 3rd (i.e., 75%) quartile. The interquartile range can be calculated as (Rousseeuw et
 355 al., 1999):

$$\Delta Q = Q3 - Q1, \quad (3)$$

356 where the lowest and highest data are in the range of $Q1 - 1.5\Delta Q$ to $Q3 + 1.5\Delta Q$ (Tukey,
 357 1977). Any data beyond this range are regarded as outliers. In this study, box plots are used
 358 to analysis the relationship between rainfall and groundwater storage.

359 3.2.4. Cross-correlation analysis

360 Cross correlation is a standard method of evaluating the similarity to which two series are
 361 linearly correlated. Assuming there are two series x_i and y_i , where $i = 0, 1, 2, \dots$, the correlation
 362 r at delay d is defined as (Bourke, 1996):

$$r = \frac{\sum_i (x_i - \bar{x})(y_i - \bar{y})}{\sqrt{\sum_i (x_i - \bar{x})^2} \sqrt{\sum_i (y_i - \bar{y})^2}} \quad (4)$$

363 where the \bar{x} and \bar{y} are the mean of correlated series.

364 To study the lag time and correlation of groundwater storage changes with rainfall, a corre-
 365 lation analysis is carried out between GRACE-derived ΔGW and precipitation. Also, a corre-
 366 lation analysis between GRACE and WGHM-derived ΔGW for validation purpose is presented
 367 in Supporting Material (Section A).

368 3.2.5. Comparison between aquifer recharge and discharge speeds

369 The groundwater table level will raise and fall in wet and dry seasons, respectively, consid-
 370 ering rainfall as a major source. However, different rock formations will have different recharge
 371 and discharge speeds due to the rock properties, layer structures and elevation impacts. The
 372 ‘dam’ reservoir pattern (see section 2.4 and Table 3) is such a special phenomenon, which indi-
 373 cates large potential of groundwater volume given that it has a strong ability to hold water with
 374 a rapid response of recharge, but slow rate of discharge. It is necessary, therefore, to compare
 375 the groundwater recharge rates in wet seasons to discharge in dry seasons in order to test the
 376 ability of holding groundwater in different regions. In this case, all the 138 months of ground-
 377 water changes employed are distributed and divided into increasing and decreasing parts. The
 378 values are then sorted from low to high for the increasing parts, and from high to low for the
 379 decreasing parts and plotted separately. The slopes of the increasing and decreasing parts are
 380 then compared to give recharge and discharge speeds. A single value of slope is calculated as
 381 (modified to the case of groundwater change from Sawicz et al., 2011):

$$S = \frac{\Delta GW(2/3_{rd}) - \Delta GW(1/3_{rd})}{N(2/3_{rd}) - N(1/3_{rd})}, \text{ wet season,} \quad (5)$$

$$S = \frac{\Delta GW(1/3_{rd}) - \Delta GW(2/3_{rd})}{N(2/3_{rd}) - N(1/3_{rd})}, \text{ dry season,} \quad (6)$$

382 where S , is the slope which reflects the speed of recharge (Eq. 5) and discharge (Eq. 6), ΔGW
 383 $1/3_{rd}$ is the one third value of increasing or decreasing parts, N is the data number count
 384 of increasing and decreasing part, respectively. The higher values of groundwater change in

385 slope plot may be attributed to extreme rainfall and the lower values may be subject of severe
386 drought throughout the period of analysis. For this reason, the slope is calculated in a range
387 where variation is not greatly subjected to both extremes such as between the $1/3_{rd}$ and $2/3_{rd}$
388 groundwater value in order to avoid bias.

389 4. Results and discussion

390 4.1. Spatial temporal variability of groundwater over Brazil

391 Seasonal and annual rainfall mainly control groundwater change trends (i.e., increase in
392 wet season and decrease in dry season), given that it provides a large part of the incoming
393 water. To evaluate its impact on groundwater changes over Brazil, principle component analysis
394 (PCA) was carried out (Figure 5) to infer the effect of rainfall/rock property relationships on
395 groundwater changes. Figure 5 presents the first three dominant components of rainfall, TWS
396 changes (ΔTWS) and groundwater changes (ΔGW), which explain over 90% of the variability
397 of each product.

398 In the first principle component (PC1), rainfall, ΔTWS and ΔGW capture the annual
399 signals over Brazil, with rainfall (73.4% variability) showing extreme climate in the central
400 parts of Brazil, which varies greatly (amplitude reach to 30 cm) between wet and dry seasons.
401 Nevertheless, when it goes towards the coast, such as in regions 5 and 8 (south and northeast
402 coastal areas, respectively), the amplitude becomes smaller (approximately 0 to 5 cm). For
403 ΔTWS (74.9% variability), a strong variation (amplitude from 20 to 40 cm) in northern Brazil,
404 which corresponds to regions 1, 2, 3 and partly 4 and 6 is seen. Variation in the coastal regions
405 5, 8 and 9 are rather small (amplitude from 0 to 10 cm). The results of ΔTWS basically matches
406 those of ΔGW (81.0% variability), which demonstrates the fact that groundwater comprises a
407 major part of the total water storage, and its spatial variabilities are less affected by rainfall.

408 In PC2, rainfall shows a seasonal variations (have increasing and decreasing trends in each
409 season of year) while the ΔTWS and ΔGW time series still show annual trends, which could
410 mean that seasonal rainfall variations does not affect ΔTWS and ΔGW much. Also, from
411 EOFs of rainfall (21.3% variability), opposite rainfall trends between the northern and southern
412 Brazil is noticeable, with the Amazon river (approximately) acting as the boundary. A similar
413 pattern emerges with ΔTWS (19.8% variability). This proves that rainfall will influence spatial

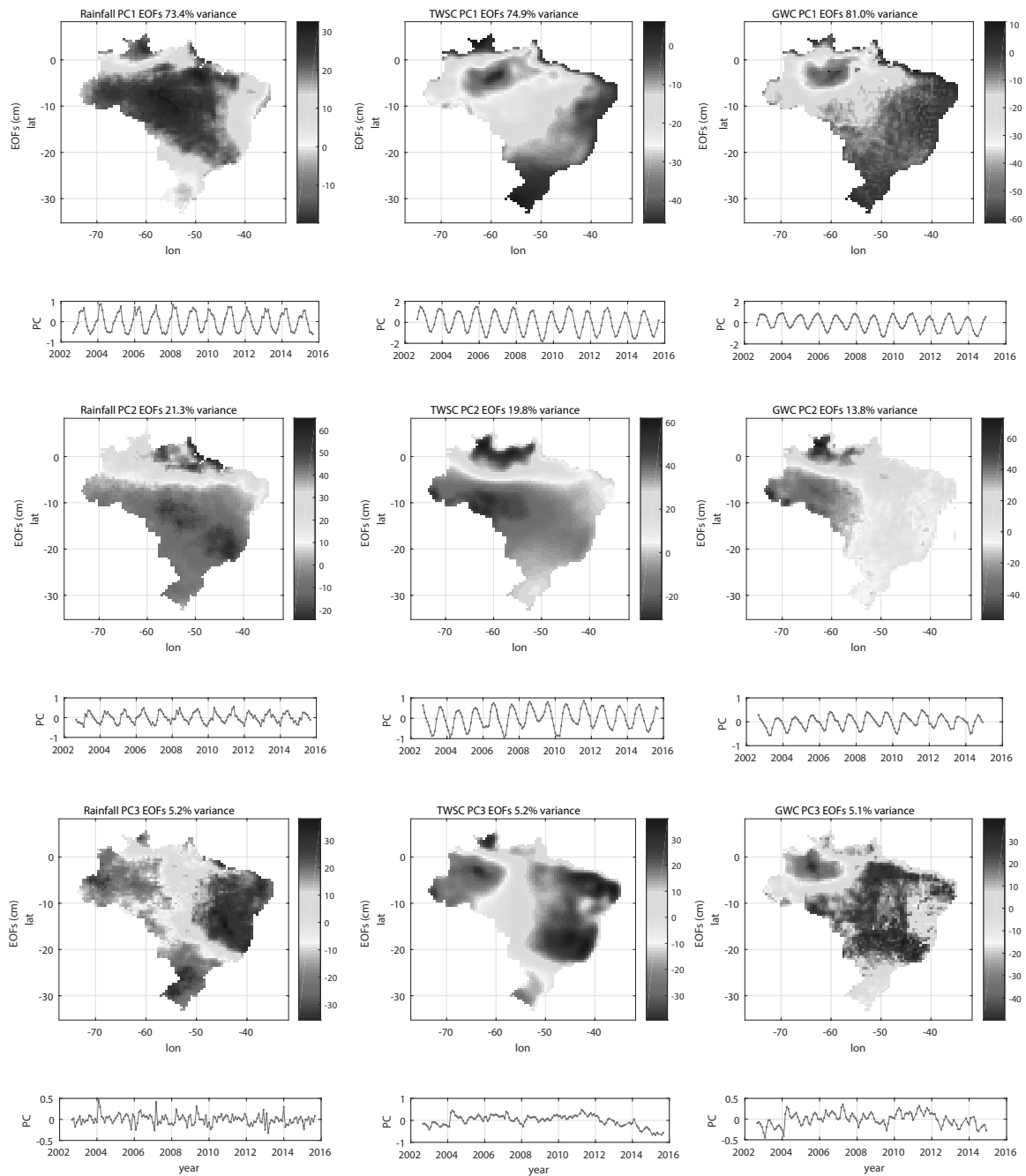


Figure 5: PCA analysis, comparison of (from left to right) rainfall, TWS, groundwater change patterns. PC1 indicates that rainfall is less affected on groundwater spatial distribution, PC2 depicts that surface water, soil moisture and canopy water are easier influenced by rainfall than groundwater, while PC3 shows the west of the west of region 2 in the Amazon basin kept losing water from 2002 to 2008.

414 distribution of surface water, soil moisture and canopy water in some extend, but has less
415 influence on groundwater. This is due to the fact that EOFs of ΔGW does not match with
416 those of rainfall and ΔTWS as seen from PC2s in Figure 5 (row 2). Besides, ΔTWS reveals
417 the droughts of 2003-2004, 2005 and 2010 that occurred in the north and northeast Brazil,
418 confirming the findings of Frappart et al. (2011) and Marengo et al. (2016). Rainfall and
419 ΔGW , however, do not show obvious signs of droughts over the same period of time. This
420 could possibly imply that those droughts affected mainly the surface water and soil moisture
421 captured by changes in TWS compared to groundwater. In addition, EOFs of ΔGW also
422 reveals that the whole region 1 (i.e., the region beyond northern side of the Amazon aquifer)
423 keeps losing water from 2002 to 2008 considering the PCs are negative mostly in the same time
424 period. This results matches well with groundwater accumulation analysis in Figure 5 in the
425 Supporting Material (Section C).

426 In PC3, the EOFs of rainfall (5.2% variability) and ΔTWS (5.2% variability) matches well,
427 with both showing that the there are opposite trends between western and eastern Brazil. More
428 importantly, in PC3, most values of the PCs in ΔTWS and ΔGW are positive from 2004 to
429 2012, which shows that the west of region 2 in the Amazon basin kept losing water during this
430 period (compare these results with those of Figure 5 in the Supporting Material, Section C).

431 4.2. Groundwater variation in relation to flow direction

432 Figure 6 shows groundwater and rainfall time series from 2002 to 2015 over the 9 study
433 regions of Brazil. As the main source of water for all regions, the rainfall changes in regions 1
434 to 4 (the Amazon region) are almost of the same amplitude compared to those of groundwater
435 changes. This is a surprising phenomenon since one would expect the amplitudes of groundwater
436 variation to be smaller than those of rainfall due to the fact that rainfall is considered to be the
437 main source of groundwater recharge. However, for regions 1 to 4, this is not the case, probably
438 due to some other significant source of water (e.g., groundwater flowing from other regions).

439 In section 2.1 (Figure 1d), a general flow direction of groundwater and surface water in
440 Brazil was presented. In region 1, there is extra groundwater coming from the north of the
441 country, from areas such as Guyana, Suriname and French Guiana. Region 2 has the biggest
442 river (the Amazon river) in Brazil, with the headstream that comes from west of Peru. Also,
443 regions 1 and 3 provide groundwater and surface water to region 2, especially for the aquifer

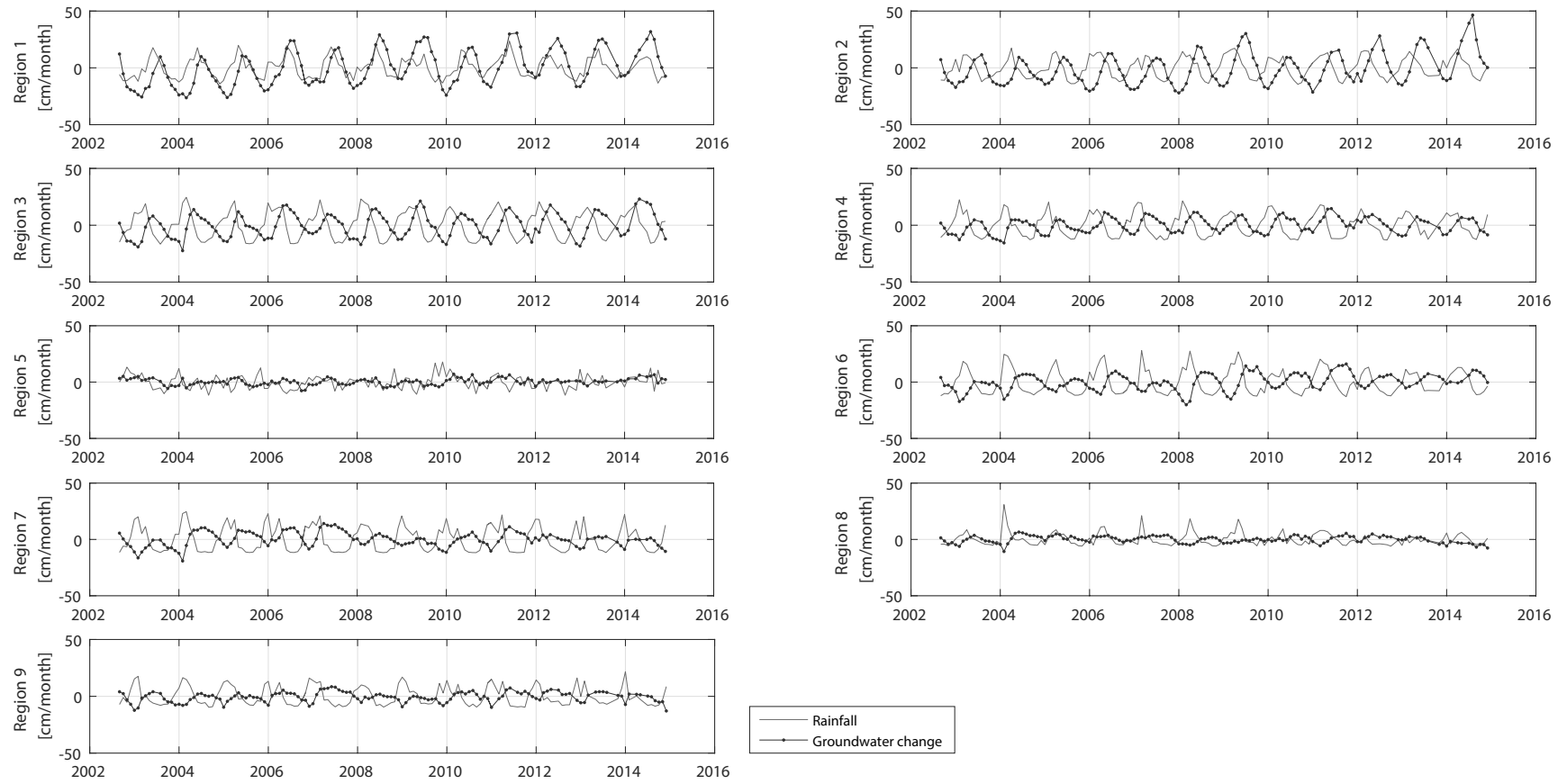


Figure 6: Time series of rainfall and groundwater changes over the study regions in Brazil. Regions 1 to 4 show that there are almost same amplitudes between rainfall and groundwater changes, which indicates these regions are receiving extra water from other regions.

444 Alter do Chão. The difference in amplitude between groundwater and rainfall in region 3 is
445 smaller compared to regions 1 and 2, which still receives extra incoming water from regions
446 4 and 7. In region 4, groundwater and rainfall variations are almost equal, with the water is
447 coming from regions 5, 7 and 9, although the quantity is a bit of small.

448 Therefore, the Amazon basin is the largest potential groundwater reservoir from the per-
449 spective of water flow in Brazil. On the other hand, rainfall and groundwater amplitudes in
450 regions 4, 6, and 7 are relatively small compared to those of regions 1 to 3, while regions 5,
451 8 and 9 have the smallest variations compared to the other regions. This is possibly due to
452 insufficient rainfall as source of groundwater and the small groundwater storage capacity of
453 those regions, which will be discussed in Section 4.3.

454 *4.3. Groundwater storage capacity*

455 Rainfall, as main source of groundwater, determines groundwater storage to a large extend,
456 unless the storage capacity of areas are very small due to the limitation of rock properties.
457 To identify the groundwater storage capacity of each region, rainfall and groundwater changes
458 are compared in Figure 7. Also, Table 5 combines the geological properties and groundwater
459 changes for a convenient view to identify groundwater storage capacity (the ability to hold
460 groundwater will be discussed in Section 4.4).

461 According to Figure 7, the medium values (red lines) and box range show that regions 1,
462 2 and 3 (the Amazon region) have the highest rainfall values among all the regions about 10
463 to 20 cm. The Amazon region, therefore, can be said to have the largest groundwater storage
464 capacity over Brazil is already pointed out in Section 4.2. More specifically, regions 1 and 3 are
465 comprised of fractured rock types in which the groundwater storage conditions and capacity
466 are not expected to be stable, nor be as large as that of the granular rock formation in region 2
467 (see Table 5). However, a similar variation pattern is seen in these three regions, possibly due
468 to the fact that regions 1 and 3 display a ‘dam’ pattern, as discussed in Section 4.4. The range
469 of medium rainfall values in regions 4, 5, 6 and 7 are from 10 to 15 cm. Regions 8 and 9 along
470 the coastal areas have the smallest medium rainfall values (approx. 5 to 10 cm). One can see
471 that although region 5 (part of the Guarani aquifer) has the smallest groundwater variation,
472 its rainfall is higher than in regions 8 and 9 (lower groundwater change regions, see Figure
473 6). By reviewing Section 2.3 and Figure 1b, it is not hard to see that the very limited direct

474 recharge area (Botucatu and Piramboia layers exposed on the surface) is the reason why the
 475 groundwater water variation in region 5 is so small and stable. To more accurately evaluate
 476 region 5's groundwater volume, in-situ data, such as water table height time series observed
 477 from local wells, are needed. Meanwhile, regions 8 and 9 have low groundwater storage capacity
 478 due the fact that they have low rainfall recharge (see Figure 7).

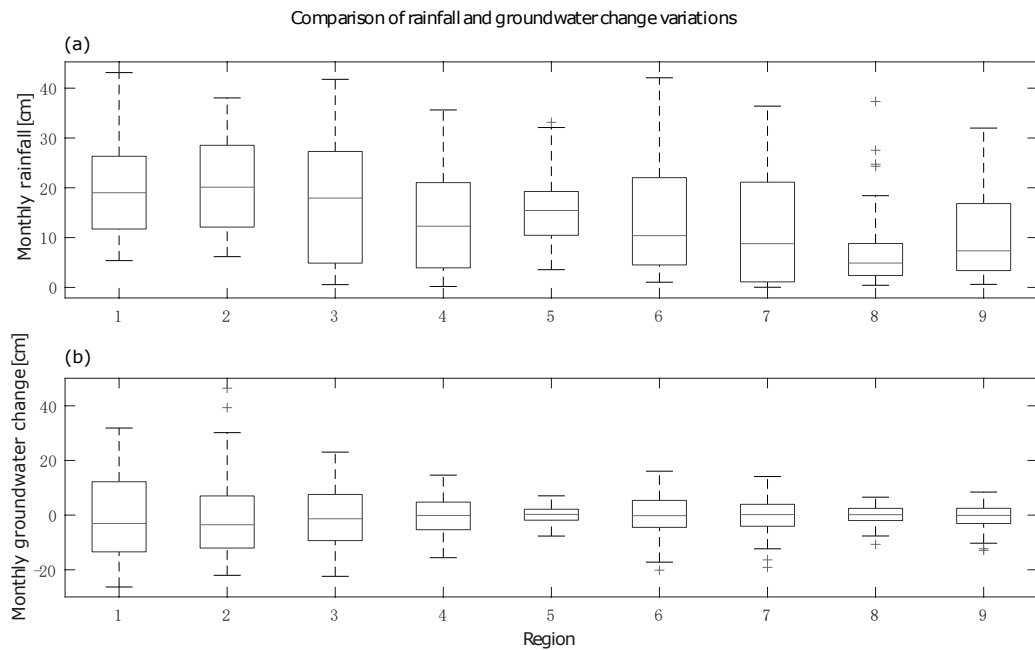


Figure 7: Comparison of monthly rainfall and groundwater changes over the study region. The red crosses indicates outliers. The lower tail of the box plots indicate the smallest observation (sample minimum), the lower end of the box shows the lower quartile (25%), the line across the box indicates the median, the upper end of the box specify the upper quartile (75%), and the upper tail of the plots illustrate the largest observations (sample maximum).

479 Comparing Tables 1 and 3, almost all the main aquifer layers in each region, except region
 480 7, belong to the granular rock types. According to Ricardo and Bruno (2011), the Urucuia
 481 aquifer in region 7 is made up of granular rocks with a permeability greater than 10^{-4} . On the
 482 one hand, although the Bambui aquifer is located in an area with vast karst terrain, consisting
 483 of limestones with extremely well developed fractures, it still provides good conditions for
 484 groundwater movement and storage capability. On the other hand, for the biggest two aquifer
 485 systems in Brazil (Amazon and Guarani aquifers), the main aquifer layers, Alter do Chão and

Table 5: Geological properties linked to groundwater changes over Brazil.

Regions	Aquifer	Rock type*	Rainfall medium (cm)	Permeability# average(m/s)	GW Variation amplitude (cm)	Ability of holding GW RS-DS ⁺
1	N/A	Fractured	20	10^{-8} to 10^{-7}	30	0.29
2	Amazon aquifer	Granular	20	$\geq 10^{-4}$	30	0.14
3	N/A	Fractured	20	10^{-8} to 10^{-7}	25	0.44
4	Guarani and Pantanal	Granular	10 to 15	$\geq 10^{-4}$	10 to 15	0.14
5	Guarani aquifer	Granular	10 to 15	10^{-6} to 10^{-4}	below 5	N/A
6	Itapecuru, Piaui	Granular	10 to 15	10^{-6} to 10^{-4}	10 to 15	0.08
7	Urucuia and Bambui	Fractured/Granular	10 to 15	$\geq 10^{-4}$	10 to 15	-0.01
8	N/A	Fractured	below 10	10^{-8} to 10^{-7}	below 5	N/A
9	N/A	Fractured	below 10	10^{-8} to 10^{-7}	below 8	N/A

Note:

1)* Regions 4 and 5 rock layers consist of both granular and fractured rocks. However, the main aquifer layers are granular rocks, so we define these aquifers as granular. Furthermore, region 7 has both granular and fractured rocks as the main aquifer formations;

2)# Permeability given in this table is only for the main rock layer that contains groundwater and the results should be interpreted with caution;

3)⁺ RS-DS is the difference between Recharge Slope (SR) and Discharge Slope (DS).

486 Botucatu & Piramboia, also have a permeability equal to or over 10^{-4} , which indicate large
487 groundwater storage potential (see Table 3).

488 4.4. *Aquifer recharge/discharge mechanism*

489 The observed lags between groundwater changes and rainfall represent the time that rainfall
490 takes to filtrate into the ground. Table 6 summarise the lags and correlations between ground-
491 water and rainfall changes over the study region (at a 95% confidence level). Higher lag periods
492 are indicative of indirect recharge mechanisms, which refers to the strong ability of holding
493 groundwater, and small storage capacity, while smaller values are more likely to be attributed
494 to direct recharge mechanisms (rapid response to rainfall and large storage capacity potential).
495 The results show that the Amazon regions 1 to 3 and region 4 have the highest correlations,
496 above 0.70, which can be attributed to the direct recharge mechanism (region 2 receives a large
497 amount of groundwater from other areas, so it should be regarded as being recharged by both
498 direct and indirect mechanisms). Regions 6, 7 and 9 have values lower than 0.70, and can be
499 regarded as being indirectly recharged. The correlations in regions 5 and 8 are the smallest,
500 with only around 0.38 and 0.29 (not significant), respectively. It seems that rainfall does not
501 influence groundwater changes in these two regions. As for the lags, region 1 has the fastest
502 groundwater response speed, which only takes one month to detect when the incoming rainfall
503 becomes groundwater. For regions 2 to 5, this is slightly longer, with lags of 3 months. The
504 coastline regions 8 and 9 have 4 months lag, while regions 6 and 7 have the longest observed
505 lags between rainfall and groundwater, i.e., 5 months. In addition, except regions 5 and 8, all
506 the correlations between rainfall and groundwater changes are above 0.5. This indicates that
507 rainfall, as main source of groundwater, controls groundwater trends to a large extend (i.e.,
508 increase in wet season and decrease in dry season).

509 In Section 2.4, the ‘dam’ reservoir pattern was defined as an area with rapid groundwater
510 increasing rates, but slow outflow. To compare the recharge and discharge speeds of ground-
511 water, Figure 8 organised all the 138 months of groundwater values by separating increasing
512 (wet seasons) and decreasing (dry seasons) parts. The slopes are then computed using Eqs.
513 5 and 6 and are presented in Table 7. The recharge/discharge slopes reflect the flow rate in
514 wet/dry seasons (increasing/decreasing parts in Figure 8). Due to the fact that regions 8 and 9
515 are located along the coastline, and their groundwater changes and the incoming rainfall very
516 small, there exists no possibility of large groundwater storage potential in these two areas. The

Table 6: Cross-correlation summary for all regions. The correlations are with respect to the lags at 95% confidence level. The none-significant correlations are marked by an asterisk*.

Regions	Rainfall vs GWC (lags/months)	Correlation	Recharge Mechanism
1	1	0.752	direct dominant
2	3	0.793	both direct and indirect dominant
3	3	0.762	direct dominant
4	3	0.732	direct dominant
5	3	0.379*	indirect dominant
6	5	0.683	indirect dominant
7	5	0.562	indirect dominant
8	4	0.286*	indirect dominant
9	4	0.567	indirect dominant

517 recharge and discharge speeds in these two regions are therefore not examined further. As for
518 region 5 (part of the Guarani aquifer), according to the PCA results presented in Figure 5 and
519 the annual variation shown in Figure 6, it is very hard to track its groundwater increasing and
520 decreasing trends due to the fact that there is obviously no annual rainfall and groundwater
521 variation trends.

522 From Figure 8 and Table 7, regions 1 and 3 performed exactly as expected (e.g., Table 3),
523 with ‘dam’ reservoir patterns of groundwater recharge slopes of 0.85 and 0.75, but 0.56 and
524 0.31 for discharge slopes, respectively. Regions 2, 4, and 6 also show good ability for holding
525 water with the difference ranging from 0.10 to 0.15 between recharge and discharge speeds.
526 This is because regions 2 and 6 are linked to the Atlantic Ocean, which plays the role of a ‘wall’
527 due to the fact that the water tables in these regions will always keep the same level with sea
528 surface level at the edges of the coastline. As for region 4, its western domain is the plateau of
529 Altiplano, with an elevation of about 2000 m. The only opening to which groundwater can flow
530 out is through the southwestern part of the region, hence its ‘dam’ reservoir pattern appearance.

531 In addition, it is important to note that for all the regions, the number of months taken for
532 the groundwater to increase part was much less than that of the number of months taken for

533 the groundwater to decrease (Figure 8). For example, regions 1, 2, 6 and 7 take about 60 to
534 65 months (about 46%) for groundwater to increase, and 73 to 78 months (about 54%) for it
535 to decrease. Greater differences appear in regions 3 and 4, which have only about 50 months
536 (about 36%) of the increasing trends from the 138 months of data sets. Therefore, even though
537 the 'dam' reservoir pattern has a strong ability to hold water, it might still keep losing water
538 every year in those regions due to lack of rainfall. Also human consumption might be another
539 important factor to lead lose of groundwater. Those hypotheses are discussed and identified
540 in the Supporting Material (see, Section C). The results show that for the Amazon regions 1
541 and 2, it kept losing groundwater from 2002 to 2008 due to lack of rainfall, while the impact of
542 human water consumption is not significant over Brazil.

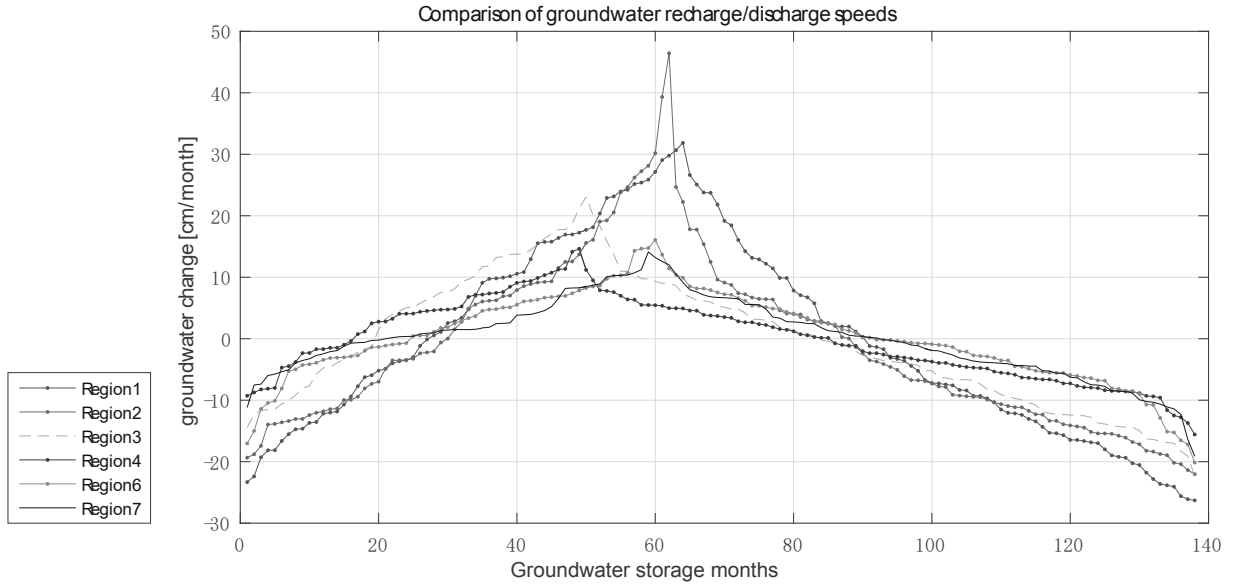


Figure 8: Comparison of recharge and discharge speeds of groundwater. Up to the 60th storage month, groundwater experiences trend of increase. Thereafter, up to the 138th month, there is a decrease (i.e., discharge).

Table 7: Recharge and discharge speed slope results based on Figure 8.

Regions	1	2	3	4	6	7
Recharge slope	0.85	0.58	0.75	0.35	0.34	0.20
Discharge slope	0.56	0.45	0.31	0.21	0.26	0.21

543 **5. Conclusion**

544 This study investigated the relationship between GRACE-derived groundwater changes and
 545 geological conditions such as rock properties and aquifer types across Brazil in order to study
 546 the groundwater potentials. By dividing the study area into 9 regions based on granular and
 547 fractured rock types, the results indicated that:

- 548 (i) From the analysis of groundwater variations and rainfall, the Amazon aquifer was found to
 549 have the largest groundwater storage capacity with the rock layers of highest permeability.

550 Guarani aquifer and east coastline inland domains follow, while coastal regions have the
551 smallest groundwater storage capacity.

552 (ii) Groundwater changes suffer less from seasonal and annual rainfall variations than total
553 water storage (TWS) over Brazil. This was evident from the Principal Component Anal-
554 ysis (PCA) results, and therefore, geological characteristics could be the main factor that
555 controls groundwater changes rates and storage capacity, rainfall, as source of groundwa-
556 ter, only controls the increasing/decreasing trends.

557 (iii) The two main aquifer formations (Alter do Chão in the Amazon aquifer, Botucatu and
558 Piramboia in the Guarani aquifer) that contribute to groundwater changes belong to the
559 granular rock type, in contrast to fractured rocks which provide more stable conditions
560 and larger space to support groundwater flow. Only the Bambui aquifer (region 7) is made
561 of fractured rocks that have large potential capacity to store groundwater.

562 (iv) Groundwater over the Amazon region was found to be not only recharged by rainfall, but
563 also inflow of groundwater from other regions.

564 (v) Although regions adjacent to the northern and southern Amazon basin do not contain
565 any aquifer system, the groundwater recharge rates in these two regions are much faster
566 than the discharge speed (defined as the ‘dam’ pattern). A large amount of groundwater
567 can not go through both northern and southern edges of Alter do Chão due to the fact
568 that there are two impermeable rock layers acting like ‘walls’, preventing water flowing
569 through them.

570 (vi) Although rainfall in Guarani aquifer is substantial, the very limited direct recharge areas
571 (Botucatu and Piramboia aquifer layers exposed at the surface) of the ‘basin’ pattern is
572 the reason that contributes to small changes in groundwater.

573 (vii) For the Amazon regions, the study found that the lose of water experienced from 2002
574 to 2008 was due to climatic variability, e.g., lack of rainfall. Geological characteristics
575 were found not to have a significant contribution in this loss. The human consumption
576 could not have significant contribution to the loss either, which had been proved by our
577 WGHM results that corroborated those of Feick et al. (2005) (see details in the Supporting
578 Material).

579 **Acknowledgements**

580 The authors are grateful to the following organizations for providing the data used in this
581 study CSR, NASA, USGS, GES-DISC, Hydro-web and CPRM Brazilian government. Many
582 thanks to Nathan, Chris and Mehdi of Curtin Universtiy for providing valuable comments
583 during data processing. Joseph and Rodrigo are grateful for the Brazilian Science Without
584 Borders Program/CAPES Grant No. 88881.068057/2014-01, which supported this study and
585 the stay of the Joseph at UFPE Federal University of Pernambuco, Brazil. Rodrigo also would
586 like to thank the support of CNPq Grant No. 310412/2015-3/PQ level 2.

587 **References**

- 588 Abelen, S., Seitz, F., Abarca-del-Rio, R., and Güntner, A. (2015). Droughts and floods in
589 the la plata basin in soil moisture data and GRACE. *Remote Sensing*, 7(6), 7324–7349,
590 doi:10.3390/rs70607324.
- 591 Alisson, E. (2014). Amazonia has an "underground ocean". Access from http://agencia.fapesp.br/amazonia_has_an_underground_ocean/19679/ on July 29, 2016.
- 593 Andersen, O. B., Seneviratne, I., Hinderer, J. and Viterbo, P. (2005). GRACE-derived terrestrial
594 water storage depletion associated with 2003 European heat wave. *Geophysical Research*
595 *Letters*, 32(18), L18405, doi:10.1029/2005GL023574.
- 596 Awange, J. L., Forootan, E., Kusche, J., Kiema, J. B. K., Omondi, P. A., Heck, B., Fleming, K.,
597 Ohanya, S. O. and Gonçalves, R. M. (2013). Understanding the decline of water storage across
598 the Ramser-Lake Naivasha using satellite-based methods. *Advances in Water Resources*, 60,
599 7–23, doi:10.1016/j.advwatres.2013.07.002.
- 600 Awange, J. L., Gebremichael, M., Forootan, E., Wakbulcho, G., Anyah, R., Ferreira, V. G.
601 and Alemayehu, T. (2014). Characterization of Ethiopian mega hydrogeological regimes
602 using GRACE, TRMM and GLDAS datasets. *Advances in Water Resources*, 74, 64–78,
603 doi:10.1016/j.advwatres.2014.07.012.
- 604 Awange, J. L., Mpelasoka, F., Goncalves, R. M. (2016). When every drop counts: Analysis of
605 Droughts in Brazil for the 1901-2013 period. *Science of the Total Environment*, 1472(88),
606 566–567, doi:10.1016/j.scitotenv.2016.06.031.
- 607 Bahniuk, A. M., Matsuda, N. S., Neto, J. M. R., Franca, A B, Jahnert R J, Juschaks, L. (2008).
608 Geological and geomorphological elements in the karst systems; Precambrian acungui group,
609 Southern Brazil. *33rd International Geological Congress*, 33. Access from <http://search.proquest.com.dbgw.lis.curtin.edu.au/> on July 21, 2016.
- 611 Birkinshaw, S. and Moore, P. (2014). CRYosat-2 sUCcess over Inland water And Land. *New-*
612 *castle University*, 1, 1–45.
- 613 Bourke, P. (1996). Cross Correlation. Access from <http://paulbourke.net/miscellaneous/correlate/> on November 13, 2016.

- 615 Broad, K., Pfaff, A., Taddei, R., Sankarasubramanian, A., Lall, U., Assis, S. F. (2007). Cli-
616 mate, stream flow prediction and water management in northeast Brazil: Societal trends and
617 forecast value. *Climatic Change*, 84(2), 217–239, doi:10.1007/s10584-007-9257-0.
- 618 Cameron, J. (2012). Groundwater Essentials. *National Water Commission*, pp. 1–48. Access
619 from http://www.groundwater.com.au/.../Groundwater_essentials.pdf on September
620 14, 2016.
- 621 Cao, Y., Nan, Z., & Cheng, G. (2015). GRACE gravity satellite observations of terrestrial water
622 storage changes for drought characterisation in the arid land of Northwest China. *Remote*
623 *Sensing*, 7(1), 1021–1047, doi:10.3390/rs70101021.
- 624 Castellazzi, P., Martel, R., Galloway, D. L., Longuevergne, L. and Rivera, A. (2016) Assessing
625 Groundwater Depletion and Dynamics Using GRACE and InSAR: Potential and Limitations.
626 *Groundwater*, pp. 1–13, doi:10.1111/gwat.12453.
- 627 Charles, J. T., William, M. A. (2001). Ground-Water-Level Monitoring and the Importance of
628 Long-Term Water-Level Data. *U.S. Geological Survey*. Access from [http://pubs.usgs.gov/
629 circ/circ1217/pdf/circ1217_final.pdf](http://pubs.usgs.gov/circ/circ1217/pdf/circ1217_final.pdf) on September 11, 2016.
- 630 CPRM. (2014). Map of Hydrogeology of Brazil. *Brazil geology service*. Accessed from [http:
631 //geobank.cprm.gov.br/](http://geobank.cprm.gov.br/) on August 17, 2016.
- 632 Cretaux, J. F., Jelinski, W., Calmant, S., et al. (2011). A lake database to monitor in the Near
633 Real Time water level and storage variations from remote sensing data. *Advances in space*
634 *Research*, 47, 1497–1507, doi:10.1016/j.asr.2011.01.004.
- 635 Döll, P., Schmied, M. C., Schuh, C., Portmann, F. T. and Eicker, A. (2014). Global-scale assess-
636 ment of groundwater depletion and related groundwater abstractions: Combining hydrologi-
637 cal modeling with information from well observations and grace satellites. *Water Resources*
638 *Research*, 50(7), 5698–5720, doi:10.1002/2014WR015595.
- 639 Döll, P., Douville, H., Güntner, A., Schmied, H. M. and Wada, Y. (2015). Modelling Freshwater
640 Resources at the Global Scale: Challenges and Prospects. *Surveys in Geophysics*, 37, 1–27,
641 doi:10.1007/s10712-015-9343-1.
- 642 Eliene, L.S., Paulo, H. F. G., Cleane, S. S. P., Marcus, P. M. B., José, G. A. D. and
643 Wilker R. R. B. (2013). Sintese da hidrogeologia nas bacias sedimentares do Amazonas e

- 644 do Solimões: Sistemas Aquíferos Ica-Solimões e Alter do Chão. *Geosciences USP*, 13(1),
645 107–117, doi:10.5327/Z1519-874X2013000100007.
- 646 Farlin, J., Drouet, L., Galle, T., ...Kies, A. (2013). Delineating spring recharge areas in a
647 fractured sandstone aquifer (Luxembourg) based on pesticide mass balance. *Hydrogeology*
648 *Journal*, 21(4), 799–812.
- 649 Feick, S., Siebert, S., and Döll, P. (2005). Global map of artificially drained agricultural areas,
650 *University of Frankfurt (Main), Germany*, Accessed from [http://www.uni-frankfurt.de/](http://www.uni-frankfurt.de/45217895/2_agricultural_drainage_map)
651 [45217895/2_agricultural_drainage_map](http://www.uni-frankfurt.de/45217895/2_agricultural_drainage_map) on October 29, 2016.
- 652 Ferreira, V. G., Gong, Z. and Andam-Akorful, S. A. (2012). Monitoring mass changes in the
653 Volta River basin using GRACE satellite gravity and TRMM precipitation, *Bol. Ciênc. Geod.*,
654 18(4), 549–563, doi:<http://dx.doi.org/10.1590/S1982-21702012000400003>.
- 655 Filho, O. A. S., Silva, A. M., Remacre, A. Z., Sancevero, S. S., McCafferty, A. E. and Per-
656 rotta, M. M. (2010). Using helicopter electromagnetic data to predict groundwater quality in
657 fractured crystalline bedrock in a semi-arid region, northeast Brazil. *Hydrogeology Journal*,
658 18(4), 905–916, doi:10.1007/s10040-010-0582-4.
- 659 Forootan, E., Rietbrok, R., Kusche, J., Sharifi, M. A., Awange, J. L., Schmidt, M., Omondi,
660 P and Famiglietti, J. (2014). Separation of large scale water storage patterns over Iran using
661 GRACE, altimetry and hydrological data. *Remote Sensing of Environment*, 140, 580–595,
662 doi:10.1016/j.rse.2013.09.025.
- 663 Frappart, F., Papa, F., Guntner, A., Werth, S., da Silva, J. S, Tomasella, J., Seyler, F.,
664 Prigent, C., Rossow., W. B., Calmant, S., Bonnet, M. P. (2011). Satellite-based estimates of
665 groundwater storage variations in large drainage basins with extensive floodplains. *Remote*
666 *Sensing of Environment*, 115, 1588–1594, doi:10.1016/j.rse.2011.02.003.
- 667 Freeze, R. A., Witherspoon, P. A. (1967). Theoretical analysis of regional groundwater flow:
668 2. Effect of water-table configuration and subsurface permeability variation. *Water resource*
669 *research*, 3(2), 623–624, doi:10.1029/WR003i002p00623.
- 670 Friedel, M. J., de, S. F., Iwashita, F., Silva, A. M., and Yoshinaga, S. (2012). Data-driven
671 modeling for groundwater exploration in fractured crystalline terrain, northeast Brazil. *Hy-*
672 *drogeology Journal*, 20(6), 1061–1080, doi:10.1007/s10040-012-0855-1.

- 673 Gastmans, D., Hutcheon, L., Menegàrio, A. A. and Chang, H. K. (2016). Geochemical evolution
674 of groundwater in a basaltic aquifer based on chemical and stable isotopic data: Case study
675 from the Northeastern portion of Serra Geral Aquifer, São Paulo state (Brazil). *Journal of*
676 *Hydrogeology*, 535, 598–611, doi:http://dx.doi.org/10.1016/j.jhydrol.2016.02.016.
- 677 Getirana, A. (2015). Extreme Water Deficit in Brazil Dected from Space. *Journal of Hydrom-*
678 *eteorology*, 17, 591–599, doi:http://dx.doi.org/10.1175/JHM-D-15-0096.1.
- 679 Han, S., Kim, H., Yeo, I., Yeh, I., Oki, T., Seo., K., Alsdorf, D. and Luthcke, S. B. (2009). Dy-
680 namics of surface water storage in the Amazon inferred from measurements of inter-satellite
681 distance change. *Geophysical Research Letters*, 36(9), doi:10.1029/2009GL037910.
- 682 Haohan, W., Xiufeng, H. and Zheng, J. (2013). Terrestrial water storage variations in Southwest
683 China revealed by gravity mission and hydrologic and climate model. *Journal of Natural*
684 *Sciences*, 41(6), 488–492.
- 685 Harter, T. (2001). Groundwater Hydrology. *California Department of Water Resources*, pp. 1-
686 2. Accessed from <http://groundwater.ucdavis.edu/files/136254.pdf> on September 9,
687 2016.
- 688 Hirata, R., Conicelli, B. P. (2012). Groundwater resources in Brazil: a review of possible im-
689 pacts caused by climate change. *Anais da Academia Brasileira de Ciencias*, 84(2), 297–312,
690 doi:http://dx.doi.org/10.1590/S0001-37652012005000037.
- 691 Hualan, R. and Hiroko, B. (2016). Global Land Data Assimilation System Version 2 (GLDAS-
692 2) Products. Accessed from [http://hydro1.sci.gsfc.nasa.gov/data/s4pa/GLDAS/GLDAS_](http://hydro1.sci.gsfc.nasa.gov/data/s4pa/GLDAS/GLDAS_NOAH10_M.2.0/doc/README_GLDAS2.pdf)
693 [NOAH10_M.2.0/doc/README_GLDAS2.pdf](http://hydro1.sci.gsfc.nasa.gov/data/s4pa/GLDAS/GLDAS_NOAH10_M.2.0/doc/README_GLDAS2.pdf) on September 22, 2016.
- 694 Huffman, G. J. and Bolvin, D. (2015). Real-Time TRMM Multi-Satellite Precipitation Analy-
695 sis Data Set Documentation. Access from: [https://pmm.nasa.gov/sites/default/files/](https://pmm.nasa.gov/sites/default/files/document_files/3B4XRT_doc_V7.pdf)
696 [document_files/3B4XRT_doc_V7.pdf](https://pmm.nasa.gov/sites/default/files/document_files/3B4XRT_doc_V7.pdf) on September 22, 2016.
- 697 Jekeli, C. (1981). Alternative methods to smooth the Earth’s gravity field. *Technical Report*,
698 Rep 327.
- 699 Kummerow, C., William, B., Toshiaki, K., James, S., and Simpson, J. (1998) The tropical
700 rainfall measuring mission (TRMM) sensor package. *Atmos Oceanic Tech*, 809, 15–17.

- 701 Landerer, F. W., and Swenson, S. C. (2012). Accuracy of scaled GRACE terrestrial water
702 storage estimates. *Water Resources Research*, 48, W045531, doi:10.1029/2011WR011453.
- 703 Lemos, M. C., Finan, T. J., Fox, R. W., Nelson, D. R. and Tucker, J. (2002). The use of seasonal
704 climate forecasting in policymaking: Lessons from northeast Brazil. *Climatic Change*, 55(4),
705 479–597, doi:10.1023/A:1020785826029.
- 706 Marengo, J. A., Torres, R. R. and Alves, L. M. (2016). Drought in Northeast Brazilpast, present,
707 and future. *Theoretical and Applied Climatology*, pp. 1-12, doi:10.1007/s00704-016-1840-8.
- 708 Marimon, M. P. C., Roisenberg, A., Suhogusoff, A. V. &Viero, A. P. (2013). Hydrogeo-
709 chemistry and statistical analysis applied to understand fluoride provenance in the guarani
710 aquifer system, southern Brazil. *Environmental Geochemistry and Health*, 35(3), 391–403,
711 doi:10.1007/s10653-012-9502-y.
- 712 Melo, D., Scanlon, B. R., Zhang, Z. and Wendland, E. (2016). Reservoir storage and hydrologic
713 responses to droughts in the Paran River Basin, Southeast Brazil. *Hydrol. Earth Syst. Sci.*
714 *Discuss*, doi:10.5194/hess-2016-258.
- 715 Mendonça, L. A., Ribeiro, Frischkorn, H., Santiago, M. F. and Filho, J. M. (2005). Isotope
716 measurements and groundwater flow modeling using MODFLOW for understanding envi-
717 ronmental changes caused by a well field in semiarid Brazil. *Environmental Geology*, 47(8),
718 1045–1053, doi:10.1007/s00254-005-1237-y.
- 719 Müller Schmeid, H., Eisner, S., Franz, D., Wattenbach, M., Portmann, F. T., Flörke, M. and
720 Döll, P. (2014). Sensitivity of simulated global-scale freshwater fluxes and storages to input
721 data, hydrological model structure, human water use and calibration. *Hydrology and Earth*
722 *System science*, 18, 3511–3538, doi:10.5194/hess-18-3511-2014.
- 723 Nanteza, J., de Linage, C. R., Thomas, B. F. and Famiglietti, J. S. Monitoring groundwater
724 storage changes in complex basement aquifers: An evaluation of the GRACE satellites over
725 East Africa. *Water Resource Research*, doi:10.1002/2016WR018846.
- 726 Negri, A. J., Adler, R. F., Xu, L. &Surratt, J. (2004). The impact of Amazonian deforestation
727 on dry season rainfall. *Climate*, 17(6), 1306–1319.
- 728 Nelson, S. A. (2015). Groundwater. *Physical Geology, EENS*, 1100.

- 729 Norbre, C. A., Marengo, J. A., Seluchi, M. E., Cuartas, L. A., Alves, L. M. (2016).
730 Some Characteristics and Impacts of the Drought and Water Crisis in Southeastern
731 Brazil during 2014 and 2015. *Journal of Water Resource and Protection*, 8(2), 252–262,
732 doi:10.4236/jwarp.2016.820.22.
- 733 Ondra, R. (2002). Geochemical and stable isotopic evolution of the Guarani Aquifer System in
734 the state of São Paulo, Brazil. *Hydrogeology Journal*, 10, 643–655.
- 735 Otto, F. E. L., Coelho, C. A. S., King, A., ...Cullen, H. (2015). Factors other than climate
736 changes, main drivers of 2014/15 water shortages in Southeast Brazil. *Bulletin of the Amer-
737 ican Meteorological Society*, 96(12), S35–S40.
- 738 Paiva, R. C. D., Buarque, D. C., Collischonn, Bonnet, M. P., Frappart, F., Calmant, S. and
739 Mendes, C. A. B. (2013). Large-scale hydrologic and hydrodynamic modeling of the Amazon
740 River basin. *Water Resources Research*, 49, 1226–1243, doi:10.1002/wrcr.20067.
- 741 Pimentel, E. T. and Hamza, V. M. (2014). Use of geothermal methods in outlining deep ground-
742 water flow systems in Paleozoic interior basins of Brazil. *Hydrogeology Journal*, 22, 107–128,
743 doi:10.1007/s10040-013-1074-0.
- 744 Preisendorfer, R. W. (1988) Principal component analysis in meteorology and oceanography.
745 *Elsevier*, New York.
- 746 Ricardo, H. and Bruno, P. C. (2011). Groundwater resources in Brazil: a review of possible
747 impacts caused by climate change. *Annals of the Brazilian Academy of Sciences*, 84(2), 297–
748 312, doi:10.1590/S0001-37652012005000037.
- 749 Rodell, M., Houser, P. R., Jambor, U., Gottschalck, J., et al. (2004) The global land data
750 assimilation system. *Bull Am Meteorol Soc*, 85, 381–94, doi:10.1175/BAMS-85-3-381.
- 751 Rousseeuw, P. J., Ruts, I. and Tukey, J. W. (1999). The Bagplot: A Bivariate Boxplot. *The
752 American Statistician*, 53(4), 382-387, doi:10.2307/2686061.
- 753 Rowland, L., Da Costa, A. C. L., Galbraith, D. R., ...Meir, P. (2015). Death from drought in
754 tropical forests is triggered by hydraulics not carbon starvation. *Nature*, 528(7580), 119-122,
755 doi:10.1038/nature15539.

- 756 Sawicz, K., Wagene, T., Sivapalan, M., Troch, P.A. and Carrillo, G. (2011). Catchment classification: empirical analysis of hydrologic similarity based on catchment function in the eastern
757 USA. *Hydrology and Earth System Sciences*, 15, 2895–2911, doi:10.5194/hess-15-2895-2011.
758
- 759 Sinha. D., Syed, T. H., Famiglietti, J. S., Reager, J. T. and Thomas, R. C. (2016). Characterizing Drought in India Using GRACE Observations of Terrestrial Water Storage Deficit.
760 *Journal of Hydrometeorology*, doi:dx.doi.org/10.1175/JHM-D-16-0047.1.
761
- 762 Soler, I. G. and Bonotto, D. M. (2015). Hydrochemical and stable isotopic (H,O,S) signatures
763 in deep groundwaters of Parana basin, Brazil. *Environmental Earth Science*, 73(1),95–113,
764 doi:10.1007/s12665-014-3397-0.
- 765 Swenson, S. and Wahr, J. (2006). Post-processing removal of correlated errors in GRACE data.
766 *Geophysical Research Letters*, 33(8), L08402, doi:10.1029/2005GL025285.
- 767 Tapley, B. D., Bettadpur, S., Ries, J.C. et al. (2004). GRACE measurements of mass variability
768 in the Earth system. *Science*, 305(5683), 503–505, doi:10.1126/science.1099192.
- 769 Tarpanelli, A., Barbetta, S., Brocca, L. and Moramarco, T. (2013). River Discharge Estimation
770 by Using Altimetry Data and Simplified Flood Routing Modeling. *Remote Sensing*, 5, 4145–
771 4162. doi:10.3390/rs5094145.
- 772 Tukey, J. W (1977). *Exploratory Data Analysis*. Addison-Wesley.
- 773 Vieceli, N., Bortolin, T. A., Mendes, L. A., Bacarim, G., Cemin, G. and Schneider, V. E. (2015).
774 Morphometric evaluation of watersheds in caxias so sul city, Brazil, using SRTM(DEM) data
775 and GIS. *Environmental Earth Science*, 73(9), 5677–5685, doi:10.1007/s12665-014-3823-3.
- 776 Wahr J, Molenaar M, Bryan F. (1998). Time variability of the Earth’s gravity field: Hydrological
777 and oceanic effects and their possible detection using GRACE. *Journal of Geophysical*
778 *Research*, 103(B12), 30205–30229.
- 779 Werth, S. and Guntner, A. (2010). Calibration analysis for water storage variability of the
780 global hydrological model WGHM. *Hydrology and Earth system science*, 14, 59–78. Available
781 at www.hydrol-earth-syst-sci.net/14/59/2010/.
- 782 William, M. A. and Leonard, F. K. (2015) Bringing GRACE Down to Earth. *Groundwater*,
783 53(6), 826–829, doi:10.1111/gwat.12379.

- 784 Xiao, R., He, X., Zhang, Y., Ferreira, V. G. & Chang, L. (2015). Monitoring Groundwater
785 Variations from Satellite Gravimetry and Hydrological Models: A Comparison with in-situ
786 Measurements in the Mid-Atlantic Region of the United States. *Remote Sensing*, 7, 686–703,
787 doi:10.3390/rs70100686.
- 788 Zagonari, F. (2010). Sustainable, just, equal, and optimal groundwater management strategies
789 to cope with climate change. Insights from Brazil. *Water Resources Management*, 24(13),
790 3731–3756, doi:10.1007/s11269-010-9630-z.
- 791 Zheng, Q. Y. and Chen, S. (2015). Review on the recent developments of terrestrial water
792 storage variations using GRACE satellite-based data. *Progress in Geophysics*, 30(6), 2603–
793 2615, doi:10.6038/pg20150619.
- 794 Zhiyong, H., Yun, P., Huili, G., ... Wenji, Z. (2015). Subregional-scale groundwater depletion
795 detected by GRACE for both shallow and deep aquifers in North China Plain. *Geophysical*
796 *Research Letters*, 42(6), 1791–1799. doi:10.1002/2014GL06249.

Supplementary material for on-line publication only

[Click here to download Supplementary material for on-line publication only: Supporting Material.pdf](#)